arXiv:1602.01558v1 [math.GT] 4 Feb 2016

POLYNOMIAL OF AN ORIENTED SURFACE-LINK DIAGRAM VIA QUANTUM A_2 INVARIANT

YEWON JOUNG

Department of Mathematics, Pusan National University,
Busan 46241, Korea
yewon112@pusan.ac.kr

SEIICHI KAMADA

Department of Mathematics, Osaka City University,
Osaka 558-8585, Japan
skamada@sci.osaka-cu.ac.jp

AKIO KAWAUCHI

Osaka City University Advanced Mathematical Institute, Osaka City University
Osaka 558-8585, Japan
kawauchi@sci.osaka-cu.ac.jp

and

SANG YOUL LEE

Department of Mathematics, Pusan National University,
Busan 46241, Korea
sangyoul@pusan.ac.kr

February 5, 2016

Abstract

It is known that every surface-link can be presented by a marked graph diagram, and such a diagram presentation is unique up to moves called Yoshikawa moves. G. Kuperberg introduced a regular isotopy invariant, called the quantum A_2 invariant, for tangled trivalent graph diagrams. In this paper, a polynomial for a marked graph diagram is defined by use of the quantum A_2 invariant and it is studied how the polynomial changes under Yoshikawa moves. The notion of a ribbon marked graph is introduced to show that this polynomial is useful for an invariant of a ribbon 2-knot.

Mathematics Subject Classification 2000: 57Q45; 57M25.
Key words and phrases: marked graph diagram; ribbon marked graph; surface-link; quantum A_2 invariant; tangled trivalent graph.

1 Introduction

A *marked graph diagram* (or *ch-diagram*) is a link diagram possibly with some 4-valent vertices equipped with markers; 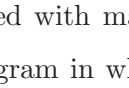 . An *oriented marked graph diagram* is a marked graph diagram in which every edge has an orientation such that each

marked vertex looks like . It is known that a surface-link is presented by a marked graph diagram (cf. [17, 21]), and such a presentation diagram is unique up to Yoshikawa moves (cf. [11, 20]). See Section 2 for details. By using marked graph diagrams, some properties and invariants of surface-links were studied in [1, 3, 4, 6, 9, 10, 13, 14, 15, 16, 19, 21].

A *tangled trivalent graph diagram* is an oriented link diagram possibly with some trivalent vertices whose incident edges are oriented all inward or all outward. In [12], G. Kuperberg introduced a regular isotopy invariant $\langle\cdot\rangle_{A_2}$, called the A_2 bracket (polynomial), for tangled trivalent graph diagrams, which is derived from the Reshetikhin-Turaev quantum invariant (cf. [18]) corresponding to the simple Lie algebra A_2.

In [15], the fourth author introduced a method of constructing invariant for a surface-link by means of a marked graph diagram and a state-sum model associated to a classical link invariant as its state evaluation. In this paper, we define a polynomial in $\mathbb{Z}[a^{-1}, a, x, y]$ for an oriented marked graph diagram by using the A_2 bracket $\langle\cdot\rangle_{A_2}$ in the line of [15] and study how the polynomial changes under Yoshikawa moves. In the process of this argument, the notion of a ribbon marked graph is introduced to show that this polynomial is useful for an invariant of a ribbon 2-knot.

This paper is organized as follows. In Section 2, we review marked graphs and their presenting surface-links. In Section 3, we recall the quantum A_2 invariant $\langle\cdot\rangle_{A_2}$ for link diagrams and tangled trivalent graph diagrams. In Section 4, we define a Laurent polynomial $\ll D \gg (a, x, y) \in \mathbb{Z}[a^{-1}, a, x, y]$ for an oriented marked graph diagram D. In Section 5, we study how the polynomial $\ll \cdot \gg$ changes under Yoshikawa moves Γ_6, Γ_6', Γ_7 and Γ_8. In Section 6, we discuss specializations of the invariant by considering some quotients of the ring $\mathbb{Z}[a^{-1}, a, x, y]$. In Section 7, the notion of a ribbon marked graph is introduced to derive an invariant of ribbon 2-knots from the polynomial. In Sections 8 and 9, we prove key lemmas used in Section 5.

2 Marked graphs and surface-links

In this section, we review marked graphs and their presenting surface-links. A *marked graph* is a spatial graph G in $\mathbb{R}^3$ which satisfies the following:

- G is a finite regular graph with 4-valent vertices, say $v_1, v_2, ..., v_n$.
- Each v_i is a rigid vertex; that is, we fix a rectangular neighborhood N_i homeomorphic to $\{(x, y) | -1 \leq x, y \leq 1\}$, where v_i corresponds to the origin and the edges incident to v_i are represented by $x^2 = y^2$.
- Each v_i has a *marker*, which is the interval on N_i given by $\{(x, 0) | -1 \leq x \leq 1\}$.

An *orientation* of a marked graph G is a choice of an orientation for each edge of G in such a way that every vertex in G looks like . A marked graph G is said to be *orientable* if it admits an orientation. Otherwise, it is said to be *non-orientable*. By an *oriented marked graph* we mean an orientable marked graph with

a fixed orientation. Two oriented marked graphs are said to be *equivalent* if they are ambient isotopic in $\mathbb{R}^3$ with keeping the rectangular neighborhoods, markers and the orientation. As usual, a marked graph can be described by a diagram in $\mathbb{R}^2$, which is a link diagram with some 4-valent vertices equipped with markers (see Figure 2).

Two marked graph diagrams present equivalent marked graphs if and only if they are related by a finite sequence of Yoshikawa moves $\Gamma_1, \Gamma_1', \Gamma_2, \Gamma_3, \Gamma_4, \Gamma_4'$ and Γ_5 depicted in Figure 1.

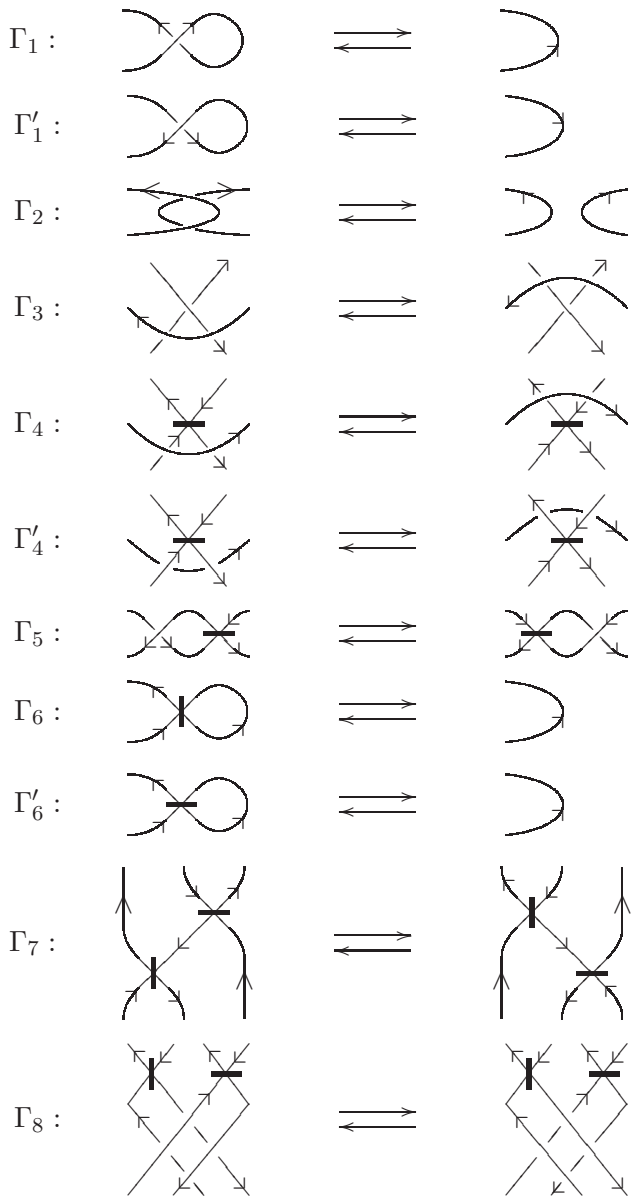

Figure 1: Yoshikawa moves

By a *surface-link* we mean a closed 2-manifold smoothly (or piecewise linearly and locally flatly) embedded in the 4-space $\mathbb{R}^4$. Two surface-links are said to be *equivalent* if they are ambient isotopic.

For a given marked graph diagram D, let $L_-(D)$ and $L_+(D)$ be classical link diagrams obtained from D by replacing each marked vertex with and , respectively (see Figure 2). We call $L_-(D)$ and $L_+(D)$ the *negative resolution* and the *positive resolution* of D, respectively. A marked graph diagram D is said to be *admissible* if both resolutions $L_-(D)$ and $L_+(D)$ are diagrams of trivial links. A marked graph is called *admissible* if its diagram is admissible.

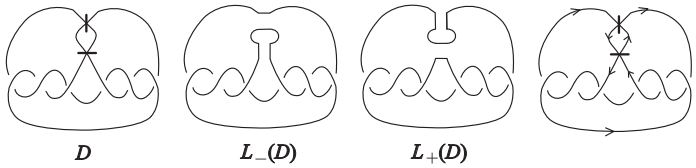

Figure 2: A marked graph diagram and its resolutions

For $t \in \mathbb{R}$, we denote by $\mathbb{R}^3_t$ the hyperplane of $\mathbb{R}^4$ whose fourth coordinate is equal to $t \in \mathbb{R}$, i.e., $\mathbb{R}^3_t := \{(x_1, x_2, x_3, x_4) \in \mathbb{R}^4 \mid x_4 = t\}$. Let $p : \mathbb{R}^4 \to \mathbb{R}$ be the projection given by $p(x_1, x_2, x_3, x_4) = x_4$. Any surface-link $\mathcal{L}$ can be deformed into a surface-link $\mathcal{L}'$, called a *hyperbolic splitting* of $\mathcal{L}$, by an ambient isotopy of $\mathbb{R}^4$ in such a way that the projection $p : \mathcal{L}' \to \mathbb{R}$ satisfies that all critical points are non-degenerate, all the index 0 critical points (minimal points) are in $\mathbb{R}^3_{-1}$, all the index 1 critical points (saddle points) are in $\mathbb{R}^3_0$, and all the index 2 critical points (maximal points) are in $\mathbb{R}^3_1$ (cf. [5, 7, 8, 17]).

Let $\mathcal{L}$ be a surface-link and let $\mathcal{L}'$ be a hyperbolic splitting of $\mathcal{L}$. The cross-section $\mathcal{L}' \cap \mathbb{R}^3_0$ at $t = 0$ is a spatial 4-valent regular graph in $\mathbb{R}^3_0$. We give a marker at each 4-valent vertex (saddle point) that indicates how the saddle point opens up above as illustrated in Figure 3.

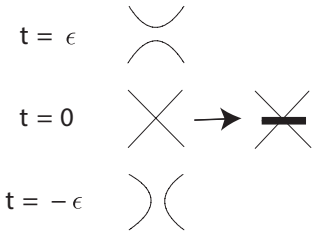

Figure 3: Marking of a vertex

The resulting marked graph G is called a *marked graph* presenting $\mathcal{L}$. Let D be a diagram of G. The diagram D is clearly admissible, which is called a *marked graph diagram* (or *ch-diagram* (cf. [19])) *presenting* $\mathcal{L}$. Conversely, any admissible marked graph presents a surface-link.

When $\mathcal{L}$ is an oriented surface-link, we choose an orientation for each edge of $\mathcal{L}' \cap \mathbb{R}^3_0$ that coincides with the induced orientation on the boundary of $\mathcal{L}' \cap \mathbb{R}^3 \times (-\infty, 0]$ by the orientation of $\mathcal{L}'$ inherited from the orientation of $\mathcal{L}$. The resulting oriented marked graph G (or its diagram D) is called an *oriented marked graph* (or an *oriented marked graph diagram*) presenting $\mathcal{L}$.

It is known that two oriented marked graph diagrams present equivalent oriented surface-links if and only if they are related by a finite sequence of 11 Yoshikawa moves shown in Figure 1 (cf. [10, 11, 20]).

3 The A_2 bracket polynomial of links and tangled trivalent graphs

In this section, we review the A_2 bracket $\langle\cdot\rangle_{A_2}$ for regular isotopy of oriented link diagrams and tangled trivalent graph diagrams derived in [12]. Although the A_2 bracket in [12] is defined such that the value for the empty diagram is 1, we here adapt another initial condition that the value of the trivial knot diagram is 1.

A *tangled trivalent graph diagram* (or an A_2 *freeway*, cf. [12]) is an oriented link diagram in S^2 possibly with some trivalent vertices whose incident edges are oriented all inward or all outward as shown in Figure 4. An example of a tangled trivalent graph diagram is in Figure 5. Throughout this paper we regard classical link diagrams as tangled trivalent graph diagrams without trivalent vertices otherwise specified. Two tangled trivalent graph diagrams are said to be *regular isotopic* if they are related by a regular isotopy, which is defined to be a sequence of operations consisting of ambient isotopy of the 2-sphere S^2 and the combinatorial moves shown in Figure 6 with all possible orientations.

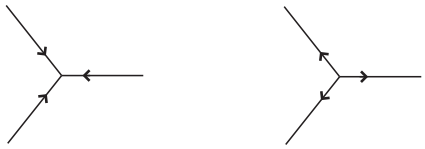

Figure 4: Trivalent vertices with orientation

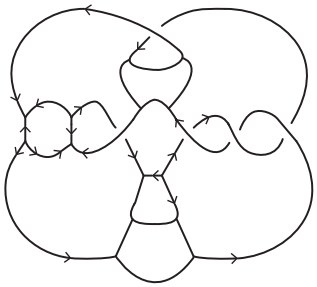

Figure 5: A tangled trivalent graph diagram

In [12], G. Kuperberg derived an inductive, combinatorial definition of a polynomial valued invariant $\langle\cdot\rangle_{A_2}$ with values in the ring $\mathbb{Z}[q^{-\frac{1}{6}}, q^{\frac{1}{6}}]$ of integral Laurent polynomials for regular isotopy classes of tangled trivalent graph diagrams. For our purpose, we present here the definition of $\langle\cdot\rangle_{A_2}$ with $q^{\frac{1}{6}} = a$. Moreover, we change the initial condition so that the trivial knot diagram has value 1.

We denote by or by O the trivial knot diagram, by O^μ the trivial link diagram with μ components, by $D \sqcup D'$ a disjoint union of diagrams D and D'.

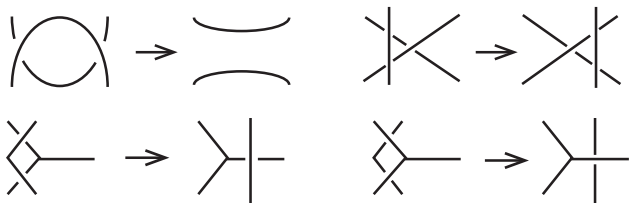

Figure 6: Moves on tangled trivalent graph diagrams

Theorem 3.1. [12, Theorem 1.2] There is an invariant $\langle\cdot\rangle_{A_2}$ with values in the ring $\mathbb{Z}[a^{-1},a]$ of integral Laurent polynomials for regular isotopy of tangled trivalent graph diagrams, called the A_2 *bracket*, which is given by the following recursive rules:

(**K0**) $\langle O\rangle_{A_2} = 1$.

(**K1**) $\langle D \sqcup O\rangle_{A_2} = (a^{-6}+1+a^6)\langle D\rangle_{A_2}$ for any diagram D.

(**K2**) $\langle$ $\rangle_{A_2} = (a^{-3}+a^3)\langle$ 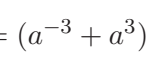 $\rangle_{A_2}$.

(**K3**) $\langle$ $\rangle_{A_2} = \langle$ $\rangle_{A_2} + \langle$ $\rangle_{A_2}$.

(**K4**) $\langle$ $\rangle_{A_2} = -a\langle$ $\rangle_{A_2} + a^{-2}\langle$ $\rangle_{A_2}$.

(**K5**) $\langle$ $\rangle_{A_2} = -a^{-1}\langle$ $\rangle_{A_2} + a^{2}\langle$ $\rangle_{A_2}$.

In [18], Reshetikhin and Turaev showed that for any simple Lie algebra $\mathfrak{g}$, there exists an invariant $RT_{\mathfrak{g}}$ of appropriately colored tangled ribbon graphs. Each edge is colored by an irreducible representation of $\mathfrak{g}$ and each vertex is colored by a tensor of a certain kind. The A_2 bracket $\langle\cdot\rangle_{A_2}$, with $\langle\emptyset\rangle_{A_2}=1$, is identically equal to $RT_{\mathfrak{g}}$ with $\mathfrak{g}=A_2$ if all edges of a tangled trivalent graph diagram are colored with the 3-dimensional representation $V_{1,0}$ whose dual is $V_{0,1}$. The colors for the vertices can be recognized as the determinant, or the usual 3-dimensional cross product. For details, see [12]. In particular, the A_2 bracket $\langle\cdot\rangle_{A_2}$ for oriented link diagrams is essentially a specialization of the HOMFLY polynomial (cf. [2]) with a normalization that makes it a regular isotopy invariant rather than an isotopy invariant. Actually, it follows from (**K4**) and (**K5**) that for any skein triple (D_+, D_-, D_0),

$$a^{-1}\langle D_+\rangle_{A_2} - a\langle D_-\rangle_{A_2} = (a^{-3}-a^3)\langle D_0\rangle_{A_2}. \tag{3.1}$$

Moreover, it is easy to check that

$$\begin{aligned}
&\langle \text{ 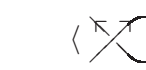 } \rangle_{A_2} = a^{-8}\langle \text{} \rangle_{A_2} = \langle \text{ 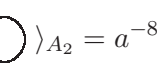 } \rangle_{A_2}, \\
&\langle \text{ 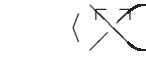 } \rangle_{A_2} = a^{8}\langle \text{} \rangle_{A_2} = \langle \text{ 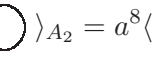 } \rangle_{A_2}.
\end{aligned} \tag{3.2}$$

4 A polynomial for oriented marked graphs via A_2 bracket

In this section, we define a polynomial invariant of oriented marked graphs using the A_2 bracket $\langle\cdot\rangle_{A_2}$ in the line of [15].

Definition 4.1. Let D be an oriented marked graph diagram or a tangled trivalent graph diagram. Let $[[D]] = [[D]](a, x, y)$ be a polynomial in $\mathbb{Z}[a^{-1}, a, x, y]$ defined by the following two axioms:

(**L1**) $[[D]] = \langle D\rangle_{A_2}$ if D is a tangled trivalent graph diagram.

(**L2**) $[[$ $]] = x[[$ $]] + y[[$ $]]$,

where , and denote the small parts of larger diagrams that are identical except the local sites indicated by the small parts.

The *writhe* $w(D)$ of an oriented marked graph diagram D is defined to be the sum of the signs of all crossings in D defined by sign $= 1$ and sign $= -1$ analogue to the writhe of a link diagram.

Definition 4.2. Let D be an oriented marked graph diagram. We define $\ll D \gg = \ll D \gg (a, x, y)$ to be a polynomial in variables a, x and y with integral coefficients given by

$$\ll D \gg = a^{8w(D)}[[D]](a, x, y).$$

Let D be an oriented marked graph diagram. A *state* of D is an assignment of T_∞ or T_0 to each marked vertex in D. Let $\mathcal{S}(D)$ be the set of all states of D. For each state $\sigma \in \mathcal{S}(D)$, let D_σ denote the oriented link diagram obtained from D by replacing marked vertices of D with two trivial 2-tangles according to the assignment T_∞ or T_0 by the state σ as follows:

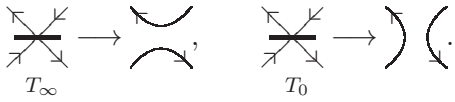

Then the skein relation (**L2**) leads the following *state-sum formula* for the polynomial $\ll D \gg$:

$$\ll D \gg = a^{8w(D)} \sum_{\sigma\in\mathcal{S}(D)} x^{\sigma(\infty)} y^{\sigma(0)} \langle D_\sigma\rangle_{A_2},$$

where $\sigma(\infty)$ and $\sigma(0)$ denote the numbers of the assignment T_∞ and T_0 of the state σ, respectively. Since $w(D) = w(D_\sigma)$ for any $\sigma \in \mathcal{S}(D)$, we also have the following formula

$$\ll D \gg = \sum_{\sigma\in\mathcal{S}(D)} x^{\sigma(\infty)} y^{\sigma(0)} \ll D_\sigma \gg . \tag{4.3}$$

Theorem 4.3. The polynomial $\ll \cdot \gg$ is an invariant for oriented marked graphs, i.e., for an oriented marked graph diagram D, the polynomial $\ll D \gg$ is invariant under Yoshikawa moves $\Gamma_1, \Gamma_1', \Gamma_2, \Gamma_3, \Gamma_4, \Gamma_4'$ and Γ_5. Moreover, it satisfies the following.

(1) $\ll O \gg = 1$.

(2) $\ll D \sqcup O \gg = (a^{-6} + 1 + a^6) \ll D \gg$ for any oriented link diagram D.

(3) $a^{-9} \ll D_+ \gg -a^9 \ll D_- \gg = (a^{-3} - a^3) \ll D_0 \gg$ for any skein triple (D_+, D_-, D_0) of link diagrams.

(4) $\ll$ $\gg = x \ll$ $\gg + y \ll$ $\gg$.

Proof. For Γ_1 and Γ_1', it follows from (3.2) that $[[$ $]] = a^{-8}[[$ $]] = [[$ $]]$. Hence, we have

$\ll$ $\gg = a^{8w($ $)}[[$ $]] = a^{8w($ $)+8}(a^{-8})[[$ $]]$

$= a^{8w($ $)}[[$ $]] = \ll$ $\gg$.

Similarly, we obtain $\ll$ $\gg = \ll$ $\gg$.

Since the A_2 bracket $\langle \cdot \rangle_{A_2}$ for oriented link diagrams (and tangled trivalent graph diagrams) and the writhe $w(D)$ are both regular isotopy invariants, $\ll \cdot \gg$ is invariant under Γ_2 and Γ_3.

The invariance of $[[\cdot]]$ under the moves Γ_4, Γ_4' and Γ_5 are seen as below, and since the writhe $w(D)$ is also invariant under these moves, we obtain the invariance of $\ll \cdot \gg$ under Γ_4, Γ_4' and Γ_5.

$[[$ 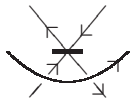 $]] = x[[$ $]] + y[[$ $]]$

$= x[[$ $]] + y[[$ 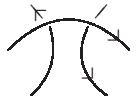 $]] = [[$ 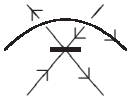 $]]$

$[[$ $]] = x[[$ $]] + y[[$ $]]$

$= x[[$ $]] + y[[$ $]] = [[$ 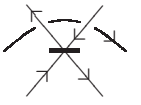 $]]$

$[[$ 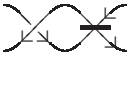 $]] = x[[$ 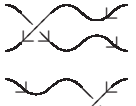 $]] + y[[$ 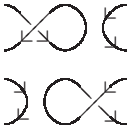 $]]$

$= x[[$ 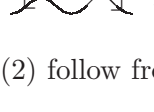 $]] + y[[$ 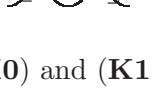 $]] = [[$ $]]$

The assertions (1) and (2) follow from (**K0**) and (**K1**).

(3) From (3.1) and (**L1**), we see

$$a^{-1}[[D_+]] - a[[D_-]] = (a^{-3} - a^3)[[D_0]].$$

Let $\lambda = w(D_0)$. Then we have

$$\begin{aligned} a^{-1}a^{8\lambda}[[D_+]] - aa^{8\lambda}[[D_-]] &= (a^{-3} - a^3)a^{8\lambda}[[D_0]], \\ a^{-9}a^{8(\lambda+1)}[[D_+]] - a^9a^{8(\lambda-1)}[[D_-]] &= (a^{-3} - a^3)a^{8\lambda}[[D_0]], \\ a^{-9} \ll D_+ \gg -a^9 \ll D_- \gg &= (a^{-3} - a^3) \ll D_0 \gg . \end{aligned}$$

(4) Clearly, $w\Big($ $\Big) = w\Big($ $\Big) = w\Big($ $\Big)$. It follows from (**L2**) that

$\ll$ $\gg = a^{8w(}$ $)[[$ 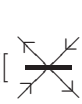 $]] = a^{8w(}$ 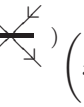 $)\Big(x[[$ $]] + y[[$ 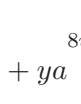 $]]\Big)$

$= xa^{8w(}$ $)[[$ $]] + ya^{8w(}$ $)[[$ $]]$

$= xa^{8w(}$ $)[[$ $]] + ya^{8w(}$ 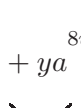 $)[[$ $]]$

$= x \ll$ 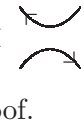 $\gg + y \ll$ $\gg .$

This completes the proof. □

Example 4.4. Here are examples of the polynomials for oriented links.

(1) $\ll$ $\gg \;\; = a^{-18} \ll O^2 \gg + (a^{-6} - a^{-12}) \ll O \gg$
$= a^{-18}(a^{-6} + 1 + a^6) + (a^{-6} - a^{-12}) = a^{-24} + a^{-18} + a^{-6}.$

(2) $\ll$ $\gg \;\; = a^{18} \ll O^2 \gg + (a^6 - a^{12}) \ll O \gg$
$= a^{18}(a^{-6} + 1 + a^6) + (a^6 - a^{12}) = a^{24} + a^{18} + a^6.$

(3) $\ll$ 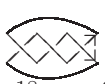 $\gg = a^{18} \ll O \gg + (a^6 - a^{12}) \ll$ $\gg$
$= a^{18} + (a^6 - a^{12})(a^{24} + a^{18} + a^6) = a^{12} + a^{24} - a^{36}.$

(4) $\ll$ $\gg = a^{-18} \ll$ $\gg + (a^{-6} - a^{-12}) \ll O \gg$
$= a^{-18}(a^{-24} + a^{-18} + a^{-6}) + (a^{-6} - a^{-12}) = a^{-42} + a^{-36} + a^{-24} - a^{-12} + a^{-6}.$

(5) $\ll$ $\gg = a^{18} \ll O \gg + (a^6 - a^{12}) \ll$ $\gg$
$= a^{18} + (a^6 - a^{12})(a^{-24} + a^{-18} + a^{-6}) = a^{-18} - a^{-6} + 1 - a^6 + a^{18}.$

(6) $\ll$ 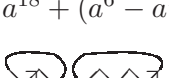 $\gg = a^{-18} \ll O \sqcup$ $\gg + (a^{-6} - a^{-12}) \ll$ $\gg$
$= (a^{-18}(a^{-6} + 1 + a^6) + a^{-6} - a^{-12})(a^{12} + a^{24} - a^{36})$
$= (a^{-24} + a^{-18} + a^{-6})(a^{12} + a^{24} - a^{36}).$

(7) $\ll$ 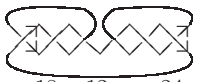 $\gg = a^{-18} \ll$ $\gg + (a^{-6} - a^{-12}) \ll$ $\gg$
$= a^{-18}(a^{12} + a^{24} - a^{36}) + (a^{-6} - a^{-12})(a^{-24} + a^{-18} + a^{-6})(a^{12} + a^{24} - a^{36})$
$= (a^{-24} + a^{-12} - a^{-36})(a^{12} + a^{24} - a^{36})$.

Example 4.5. Consider the diagram 8_1 of a spun 2-knot of the trefoil in Yoshikawa's table [21] with the orientation indicated below. From Theorem 4.3, it follows that

8_1

$\ll$ 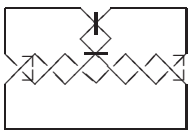 $\gg = x^2 \ll$ 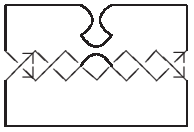 $\gg + xy \ll$ 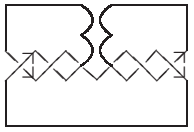 $\gg$

$+ yx \ll$ 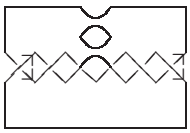 $\gg + y^2 \ll$ 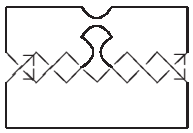 $\gg$

$= x^2 \ll O^2 \gg + xy \ll$ 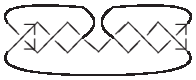 $\gg + yx \ll O^3 \gg + y^2 \ll O^2 \gg$
$= (a^{-6} + 1 + a^6)(x^2 + y^2) + (a^{-24} + a^{-12} - a^{-36})(a^{12} + a^{24} - a^{36})xy$
$+ (a^{-6} + 1 + a^6)^2 xy$.

Example 4.6. Consider the diagram 9_1 of a ribbon 2-knot associated with 6_1 knot in Yoshikawa's table [21] with the orientation indicated below.

9_1

$\ll$ 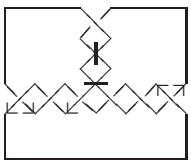 $\gg = x^2 \ll$ 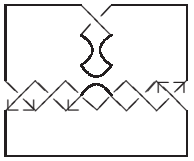 $\gg + xy \ll$ 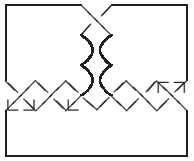 $\gg$

$+ yx \ll$ 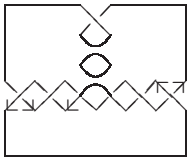 $\gg + y^2 \ll$ 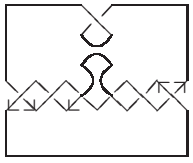 $\gg$

$= x^2 \ll O^2 \gg + xy \Big[a^{18} \ll$ $\gg + (a^6 - a^{12}) \ll$ $\gg \Big]$
$+ yx \ll O^3 \gg + y^2 \ll O^2 \gg$
$= (a^{-6} + 1 + a^6)(x^2 + y^2) + (a^{-6} + 1 + a^6)^2 xy$
$+ \Big[a^{18}(a^{-18} - a^{-6} + 1 - a^6 + a^{18}) + (a^6 - a^{12})(a^{-24} + a^{-18} + a^{-6}) \Big] xy$
$= (a^{-6} + 1 + a^6)(x^2 + y^2)$
$+ (a^{-18} + a^{-12} + a^{-6} + 5 + a^6 + a^{18} - a^{24} + a^{36})xy$.

Example 4.7. Consider the diagram 10_2 of a 2-twist spun 2-knot of the trefoil in

Yoshikawa's table [21] with the orientation indicated below.

10_2

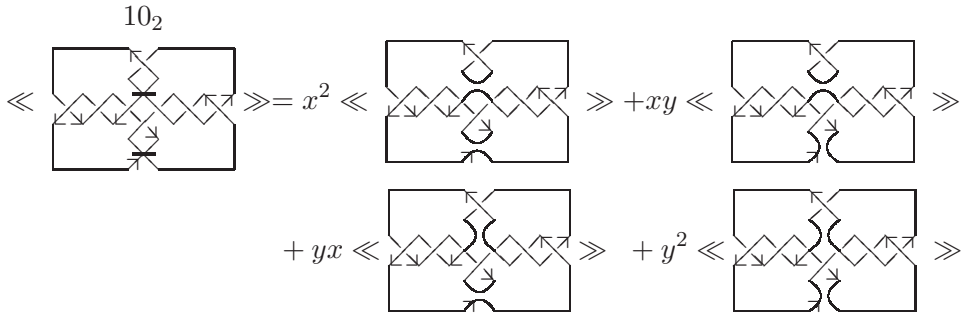

$$
\begin{aligned}
=&x^2 \ll O^2 \gg + xy\Big[a^{18} \ll O \gg + (a^6 - a^{12}) \ll \gg \Big] \\
&+ xy\Big[a^{18} \ll \gg + (a^6 - a^{12}) \ll \gg \Big] \\
&+ y^2\Big[a^{18} \ll \gg + (a^6 - a^{12}) \ll O \gg \Big] \\
=&x^2(a^{-6} + 1 + a^6) + xy\Big[a^{18} + (a^6 - a^{12})(a^{-42} + a^{-36} + a^{-24} - a^{-12} + a^{-6})\Big] \\
&+ xy\Big[a^{18}(a^{-18} - a^{-6} + 1 - a^6 + a^{18}) + (a^6 - a^{12})(a^{-24} + a^{-18} + a^{-6})\Big] \\
&+ y^2\Big[a^{18}(a^{-24} + a^{-18} + a^{-6}) + (a^6 - a^{12})\Big] \\
=&(a^{-6} + 1 + a^6)(x^2 + y^2) \\
&+ (a^{-36} - a^{-24} + 2a^{-18} - a^{-12} - 2a^{-6} + 4 - 2a^6 - a^{12} + 2a^{18} - a^{24} + a^{36})xy.
\end{aligned}
$$

5 Behaviors under Yoshikawa moves Γ_6, Γ_6', Γ_7 and Γ_8

In this section we investigate behaviors of $\ll \cdot \gg$ under Yoshikawa moves Γ_6, Γ_6', Γ_7 and Γ_8.

Proposition 5.1. The moves Γ_6 and Γ_6' change the polynomial $\ll \cdot \gg$ as follows.

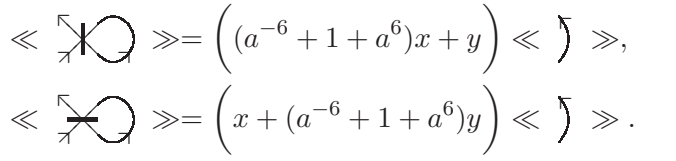

$$
\ll \quad \gg = \Big((a^{-6} + 1 + a^6)x + y\Big) \ll \quad \gg,
$$

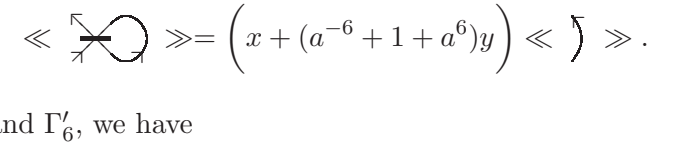

$$
\ll \quad \gg = \Big(x + (a^{-6} + 1 + a^6)y\Big) \ll \quad \gg .
$$

Proof. For Γ_6 and Γ_6', we have

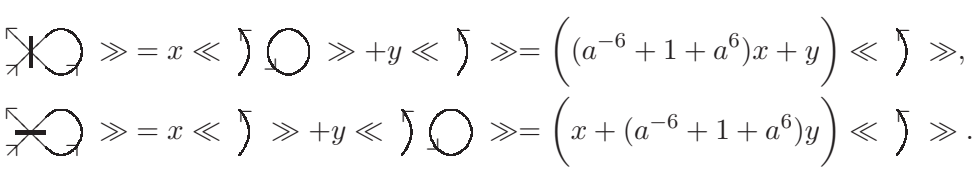

$$
\ll \quad \gg = x \ll \quad \gg + y \ll \quad \gg = \Big((a^{-6} + 1 + a^6)x + y\Big) \ll \quad \gg,
$$

$$
\ll \quad \gg = x \ll \quad \gg + y \ll \quad \gg = \Big(x + (a^{-6} + 1 + a^6)y\Big) \ll \quad \gg .
$$

This completes the proof. □

In order to consider behaviors of the polynomial $\ll \cdot \gg$ under Yoshikawa moves Γ_7 and Γ_8, we prepare lemmas.

By an *n-tangle diagram* ($n \geq 1$) we mean an oriented link diagram or a tangled trivalent graph diagram $\mathcal{T}$ in the rectangle $I^2 = [0,1] \times [0,1]$ in $\mathbb{R}^2$ such that $\mathcal{T}$ transversely intersect with $(0,1) \times \{0\}$ and $(0,1) \times \{1\}$ in n distinct points, respectively, called the *endpoints* of $\mathcal{T}$. The *boundary* of an n-tangle diagram $\mathcal{T}$ is defined to be the boundary of I^2 together with the $2n$ endpoints equipped with inward or outward pointing normals that coincide with the orientations on intersecting arcs of $\mathcal{T}$. In Figure 7, (a) is the boundary of a 3-tangle diagram, and (b) is the boundary of a 4-tangle diagram.

(a) (b)

Figure 7: Boundaries of $3, 4$-tangle diagrams

Lemma 5.2. Let $\mathcal{T}$ be a 3-tangle diagram with the boundary (a) in Figure 7 such that there are no crossings, 2-gons and 4-gons and that there are no connected components as diagrams in $\mathrm{Int}D^2$. Then $\mathcal{T}$ is one of the six fundamental 3-tangle diagrams $f_0, f_1, \ldots, f_5$ shown in Figure 8.

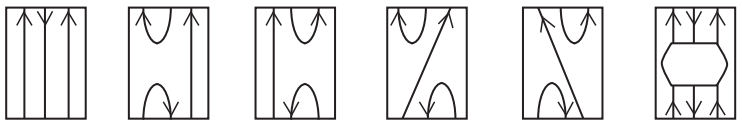

Figure 8: Fundamental 3-tangle diagrams

Lemma 5.3. Let $\mathcal{T}$ be a 4-tangle diagram with the boundary (b) in Figure 7 such that there are no crossings, 2-gons and 4-gons and that there are no connected components as diagrams in $\mathrm{Int}D^2$. Then $\mathcal{T}$ is one of the 23 fundamental 4-tangle diagrams $g_0, g_1, \ldots, g_{22}$ shown in Figure 9.

Lemmas 5.2 and 5.3 are proved in the end of this paper.

The following proposition gives the behavior of the polynomial $\ll \cdot \gg$ under a Yoshikawa move Γ_7.

Proposition 5.4. Let D and D' be oriented marked graph diagrams such that D' is obtained from D by a Yoshikawa move Γ_7 as depicted in Figure 10. Then

$$\ll D \gg - \ll D' \gg = \Delta(a)xy\psi(a,x,y),$$

where $\psi(a,x,y)$ is a polynomial in $\mathbb{Z}[a^{-1}, a, x, y]$ and

$$\Delta(a) \ := \ (a^{-6} + 1 + a^6)^2 - 1 \ = \ a^{-12}(a^{12}+1)(a^6+1)^2. \tag{5.4}$$

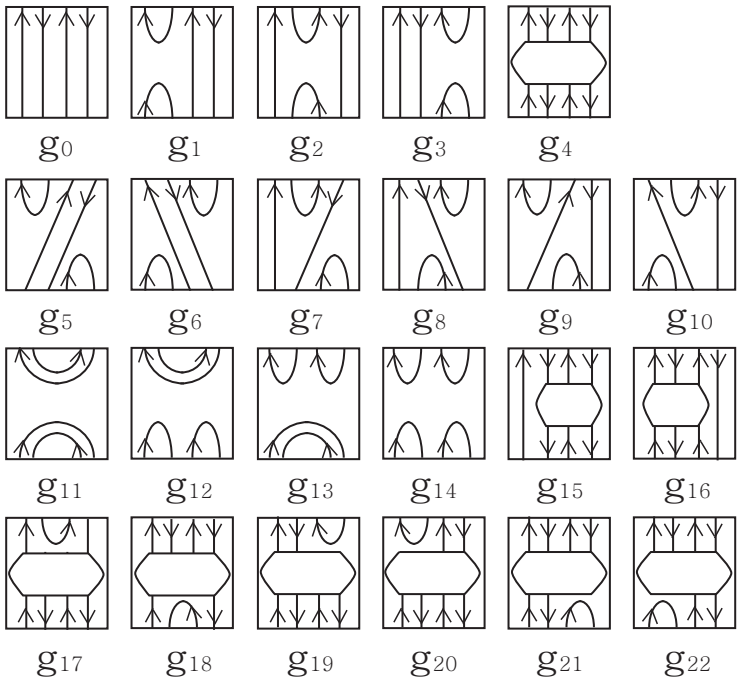

Figure 9: Fundamental 4-tangle diagrams

Proof. Applying the axioms (**L1**) and (**L2**) in Definition 4.1 and (**K1**)–(**K5**) in Definition 3.1 to the 3-tangle diagram $\mathcal{T}$ in $D = T_7 \circ \mathcal{T}$, we can express $[[D]]$ as a linear combination of polynomials $[[T_7 \circ U_k]](1 \leq k \leq m)$ for some integer $m \geq 1$, where each U_k is a 3-tangle diagram satisfying the assumption on $\mathcal{T}$ in Lemma 5.2. By the lemma, we see that U_k is one of the fundamental 3-tangle diagrams $f_0, f_1, \ldots, f_5$ in Figure 8. Hence we have

$$[[D]] = [[T_7 \circ \mathcal{T}]] = \sum_{i=0}^{5} \psi_i(a, x, y)[[T_7 \circ f_i]],$$

where $\psi_i(a, x, y)$ is a polynomial in $\mathbb{Z}[a, a^{-1}, x, y]$. Similarly, we have

$$[[D']] = [[T_7' \circ \mathcal{T}]] = \sum_{i=0}^{5} \psi_i(a, x, y)[[T_7' \circ f_i]].$$

This gives

$$[[D]] - [[D']] = \sum_{i=0}^{5} \psi_i(a, x, y)\Big([[T_7 \circ f_i]] - [[T_7' \circ f_i]] \Big). \tag{5.5}$$

By a straightforward computation, we obtain

$$[[T_7 \circ f_i]] = [[f_2 \circ f_i]]x^2 + [[f_0 \circ f_i]]xy + [[f_4 \circ f_i]]yx + [[f_1 \circ f_i]]y^2,$$
$$[[T_7' \circ f_i]] = [[f_2 \circ f_i]]x^2 + [[f_0 \circ f_i]]xy + [[f_3 \circ f_i]]yx + [[f_1 \circ f_i]]y^2.$$

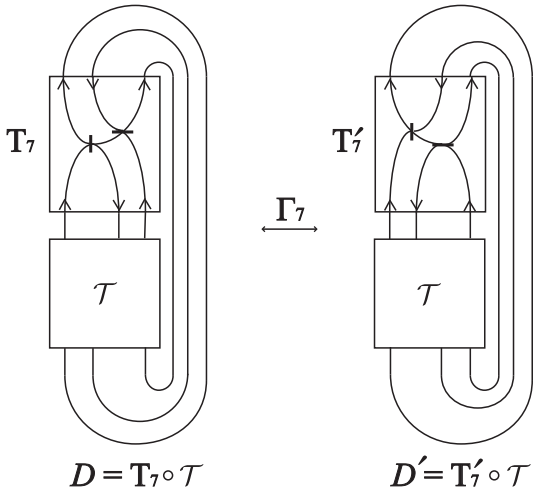

Figure 10: Yoshikawa move Γ_7

Let $A = a^{-6} + 1 + a^6$ and $B = a^{-3} + a^3$. Then it is easily checked that $[[f_3 \circ f_i]]$ and $[[f_4 \circ f_i]]$ with $0 \leq i \leq 5$ are as in Table 1. Hence

$$[[T_7 \circ f_i]] - [[T_7' \circ f_i]] = xy\Big([[f_4 \circ f_i]] - [[f_3 \circ f_i]]\Big)$$
$$= \begin{cases} 0, & i = 0, 1, 2, 5; \\ xy(A^2 - 1) = xy\Delta(a), & i = 3; \\ -xy(A^2 - 1) = -xy\Delta(a), & i = 4. \end{cases}$$

Therefore it follows from (5.5) that $[[D]] - [[D']] = \Delta(a)xy\psi'(a, x, y)$, where $\psi'(a, x, y) = \psi_3(a, x, y) - \psi_4(a, x, y)$. Finally, since $w(D) = w(D')$, we obtain $\ll D \gg - \ll D' \gg = \Delta(a)xy\psi(a, x, y)$, where $\psi(a, x, y) = a^{8w(D)}\psi'(a, x, y)$. □

$\circ$	f_0	f_1	f_2	f_3	f_4	f_5
f_3	1	A	A	1	A^2	B^3
f_4	1	A	A	A^2	1	B^3

Table 1: $[[f_3 \circ f_i]]$ and $[[f_4 \circ f_i]]$

Now we investigate the behavior of $\ll \cdot \gg$ under a Yoshikawa move Γ_8.

Proposition 5.5. Let D and D' be oriented marked graph diagrams such that D' is obtained from D by a Yoshikawa move Γ_8 as depicted in Figure 11. Then

$$\ll D \gg - \ll D' \gg = (a^{-3} - a^3)\Delta(a)xy\varphi(a, x, y),$$

where $\varphi(a, x, y)$ is a polynomial in $\mathbb{Z}[a^{-1}, a, x, y]$ and $\Delta(a)$ is the polynomial in (5.4).

Proof. Applying the axioms (**L1**), (**L2**) and (**K1**)–(**K5**) to the 4-tangle diagram $\mathcal{T}$ in $D = T_8 \circ \mathcal{T}$, we can express $[[D]]$ as a linear combination of $[[T_8 \circ V_k]] (1 \leq k \leq m)$ for

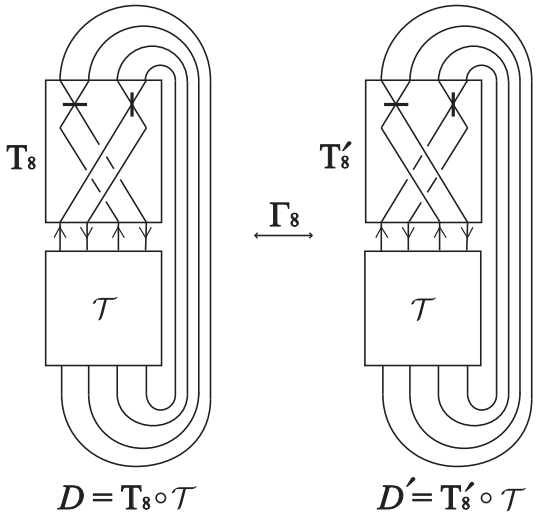

Figure 11: Yoshikawa move Γ_8

some integer $m \geq 1$, where each V_k is a 4-tangle diagram satisfying the assumption on $\mathcal{T}$ in Lemma 5.3. By the lemma, we see that V_k is one of the fundamental 4-tangle diagrams $g_0, g_1, \ldots, g_{22}$ in Figure 9. Hence we have

$$[[D]] = [[T_8 \circ \mathcal{T}]] = \sum_{i=0}^{22} \varphi_i(a,x,y)[[T_8 \circ g_i]],$$

where $\varphi_i(a,x,y) \in \mathbb{Z}[a^{-1},a,x,y]$. Similarly, we obtain

$$[[D']] = [[T'_8 \circ \mathcal{T}]] = \sum_{i=0}^{22} \varphi_i(a,x,y)[[T'_8 \circ g_i]].$$

This gives

$$[[D]] - [[D']] = \sum_{i=0}^{22} \varphi_i(a,x,y)\Big([[T_8 \circ g_i]] - [[T'_8 \circ g_i]]\Big). \tag{5.6}$$

By a straightforward computation, we obtain

$$\begin{aligned}
[[T_8 \circ g_i]] &= [[g_5 \circ g_i]]x^2 + [[g_{14} \circ g_i]]xy + [[g \circ g_i]]yx + [[g_6 \circ g_i]]y^2,\\
[[T'_8 \circ g_i]] &= [[g_5 \circ g_i]]x^2 + [[g_{14} \circ g_i]]xy + [[g^* \circ g_i]]yx + [[g_6 \circ g_i]]y^2,
\end{aligned}$$

where g and g^* are 4-tangle diagrams shown in Figure 12.

Figure 12: 4-tangle diagrams g and g^*

Using (**L1**) and (**K2**)–(**K5**), we obtain

$$\begin{aligned}[[g \circ g_i]] = a^{-6}[[g_0 \circ g_i]] + [[g_2 \circ g_i]] + [[g_4 \circ g_i]] + [[g_7 \circ g_i]] + [[g_8 \circ g_i]] \\ + [[g_9 \circ g_i]] + [[g_{10} \circ g_i]] + a^{6}[[g_{11} \circ g_i]] - a^{-3}[[g_{15} \circ g_i]] \\ - a^{-3}[[g_{16} \circ g_i]] - a^{3}[[g_{17} \circ g_i]] - a^{3}[[g_{18} \circ g_i]].\end{aligned}$$

Since g^* is the mirror image of g, it is seen from (**K4**) and (**K5**) that

$$\begin{aligned}[[g^* \circ g_i]] = a^{6}[[g_0 \circ g_i]] + [[g_2 \circ g_i]] + [[g_4 \circ g_i]] + [[g_7 \circ g_i]] + [[g_8 \circ g_i]] \\ + [[g_9 \circ g_i]] + [[g_{10} \circ g_i]] + a^{-6}[[g_{11} \circ g_i]] - a^{3}[[g_{15} \circ g_i]] \\ - a^{3}[[g_{16} \circ g_i]] - a^{-3}[[g_{17} \circ g_i]] - a^{-3}[[g_{18} \circ g_i]].\end{aligned}$$

This gives that

$$\begin{aligned}[[g \circ g_i]] - [[g^* \circ g_i]] = (a^{-3} - a^{3})\Big[(a^{-3} + a^{3})\Big([[g_0 \circ g_i]] - [[g_{11} \circ g_i]]\Big) \\ - [[g_{15} \circ g_i]] - [[g_{16} \circ g_i]] + [[g_{17} \circ g_i]] + [[g_{18} \circ g_i]]\Big].\end{aligned}$$

By simple, but tedious calculations, we obtain Table 2 for $[[g_k \circ g_i]]$ with $k = 0, 11, 15, 16, 17, 18$ and $0 \le i \le 22$.

$\circ$	g_0	g_{11}	g_{15}	g_{16}	g_{17}	g_{18}
g_0	A^3	A	AB^3	AB^3	B^3	B^3
g_1	A^2	1	B^3	AB^3	B^3	B^3
g_2	A^2	A^2	AB^3	AB^3	AB^3	AB^3
g_3	A^2	1	AB^3	B^3	B^3	B^3
g_4	B^4	B^4	$2B^3 + B^5$	$2B^3 + B^5$	$2B^3 + B^5$	$2B^3 + B^5$
g_5	1	1	B^3	B^3	B^3	B^3
g_6	1	1	B^3	B^3	B^3	B^3
g_7	A	A	AB^3	B^3	B^3	AB^3
g_8	A	A	AB^3	B^3	AB^3	B^3
g_9	A	A	B^3	AB^3	AB^3	B^3
g_{10}	A	A	B^3	AB^3	B^3	AB^3
g_{11}	A	A^3	B^3	B^3	AB^3	AB^3
g_{12}	1	A^2	B^3	B^3	B^3	AB^3
g_{13}	1	A^2	B^3	B^3	AB^3	B^3
g_{14}	A	A	B^3	B^3	B^3	B^3
g_{15}	AB^3	B^3	$2AB^2 + AB^4$	$2B^4$	$2B^4$	$2B^4$
g_{16}	AB^3	B^3	$2B^4$	$2AB^2 + AB^4$	$2B^4$	$2B^4$
g_{17}	B^3	AB^3	$2B^4$	$2B^4$	$2B^4$	$2AB^2 + AB^4$
g_{18}	B^3	AB^3	$2B^4$	$2B^4$	$2AB^2 + AB^4$	$2B^4$
g_{19}	B^3	B^3	$2B^4$	$2B^2 + B^4$	$2B^4$	$2B^2 + B^4$
g_{20}	B^3	B^3	$2B^2 + B^4$	$2B^4$	$2B^4$	$2B^2 + B^4$
g_{21}	B^3	B^3	$2B^4$	$2B^2 + B^4$	$2B^2 + B^4$	$2B^4$
g_{22}	B^3	B^3	$2B^2 + B^4$	$2B^4$	$2B^2 + B^4$	$2B^4$

Table 2: $[[g_k \circ g_i]]$

Thus it follows from (5.6) and the identity $B^2 = A + 1$ that

$$\begin{aligned}
&[[T_8 \circ g_i]] - [[T'_8 \circ g_i]] = ([[g \circ g_i]] - [[g^* \circ g_i]])xy \\
&= \begin{cases} (a^{-6} - a^6)(A-2)(A-1)(A+1)xy, & i = 0; \\ -(a^{-6} - a^6)(A-2)(A-1)(A+1)xy, & i = 11; \\ -(a^{-3} - a^3)(A-1)(A+1)xy, & i = 15, 16; \\ (a^{-3} - a^3)(A-1)(A+1)xy, & i = 17, 18; \\ 0 & \text{otherwise.} \end{cases} \\
&= \begin{cases} (a^{-3} + a^3)(a^{-6} - 1 + a^6)(a^{-3} - a^3)\Delta(a)xy, & i = 0; \\ -(a^{-3} + a^3)(a^{-6} - 1 + a^6)(a^{-3} - a^3)\Delta(a)xy, & i = 11; \\ -(a^{-3} - a^3)\Delta(a)xy, & i = 15, 16; \\ (a^{-3} - a^3)\Delta(a)xy, & i = 17, 18; \\ 0 & \text{otherwise.} \end{cases}
\end{aligned}$$

Therefore it follows from (5.6) that

$$[[D]] - [[D']] = (a^{-3} - a^3)\Delta(a)xy\varphi'(a, x, y),$$

for a polynomial $\varphi'(a, x, y)$ in $\mathbb{Z}[a^{-1}, a, x, y]$. Since $w(D) = w(D')$, we obtain

$$\ll D \gg - \ll D' \gg = (a^{-3} - a^3)\Delta(a)xy\varphi(a, x, y),$$

where $\varphi(a, x, y) = a^{8w(D)}\varphi'(a, x, y)$. □

Theorem 5.6. Let $\mathcal{L}$ be an oriented surface-link and let D be an oriented marked graph diagram presenting $\mathcal{L}$. Then the polynomial $\ll D \gg \in \mathbb{Z}[a^{-1}, a, x, y]$, modulo the ideal generated by $\Delta(a)$, is an invariant of $\mathcal{L}$ up to multiplication by powers of $(a^{-6} + 1 + a^6)x + y$ and $x + (a^{-6} + 1 + a^6)y$.

Proof. It follows from Theorem 4.3 and Propositions 5.1, 5.4 and 5.5. □

6 Specializations of the polynomial $\ll \cdot \gg$

Here we consider some specializations of the polynomial $\ll \cdot \gg$.

Let m be a non-negative integer and let $I(a^m+1)$ be the ideal $(a^m+1)\mathbb{Z}[a^{-1}, a, x, y]$ of $\mathbb{Z}[a^{-1}, a, x, y]$ generated by $a^m + 1$. We abbreviate $f + I(a^m + 1)$ as f for $f \in \mathbb{Z}[a^{-1}, a, x, y]$ unless it makes confusion.

For an oriented marked graph diagram D, we denote by $\ll D \gg_{a^m+1}$ the polynomial $\ll D \gg$ modulo the ideal $I(a^m + 1)$, i.e.,

$$\ll D \gg_{a^m+1} \;=\; \ll D \gg + I(a^m + 1) = \;\ll D \gg\; \in \mathbb{Z}[a^{-1}, a, x, y]/I(a^m + 1).$$

It follows from Theorem 4.3 that $\ll \cdot \gg_{a^m+1}$ is an invariant for oriented marked graphs satisfying the same conditions with (1)–(4) in Theorem 4.3. In particular, for any positive integer μ and for any skein triple (D_+, D_-, D_0) of link diagrams,

$$\ll O^\mu \gg_{a^m+1} = (a^{-6} + 1 + a^6)^{\mu-1} \tag{6.7}$$

and

$$a^{-9} \ll D_+ \gg_{a^m+1} - a^9 \ll D_- \gg_{a^m+1} = (a^{-3} - a^3) \ll D_0 \gg_{a^m+1} . \tag{6.8}$$

First we are interested in a case that $m = 6$ or $m = 12$, since if $a^6 + 1 = 0$ or $a^{12} + 1 = 0$ then $\Delta(a) = 0$, where $\Delta(a)$ is the polynomial in (5.4).

Suppose $m = 6$. Then, (6.7) implies that for any positive integer μ,

$$\ll O^\mu \gg_{a^6+1} = (-1)^{\mu-1}. \tag{6.9}$$

Since a^3 is a unit in $\mathbb{Z}[a^{-1}, a, x, y]/I(a^6 + 1)$, (6.8) implies that for any skein triple (D_+, D_-, D_0) of link diagrams,

$$\ll D_+ \gg_{a^6+1} + \ll D_- \gg_{a^6+1} = -2 \ll D_0 \gg_{a^6+1} . \tag{6.10}$$

Lemma 6.1. Let D be an oriented link diagram and let $\#D$ denote the number of components of the link presented by D. Then $\ll D \gg_{a^6+1}$ is 1 if $\#D$ is odd, or -1 if $\#D$ is even, i.e., $\ll D \gg_{a^6+1} = (-1)^{\#D-1}$.

Proof. When we restrict $\ll \cdot \gg_{a^6+1}$ to the family of oriented link diagrams, it is an oriented link invariant satisfying (6.9) and (6.10). On the other hand, $(-1)^{\#D-1}$ is also such an invariant. We see that $\ll D \gg_{a^6+1} = (-1)^{\#D-1}$ for any link diagram D by considering a skein tree. □

Example 6.2. Consider the diagram 8_1 of a spun trefoil in Yoshikawa's table [21]. From Lemma 6.1, it follows that

8_1

$\ll$ 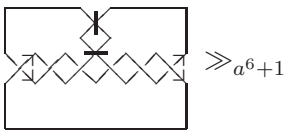 $\gg_{a^6+1}$

$= x^2 \ll$ 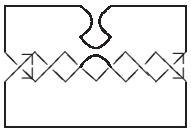 $\gg_{a^6+1} + xy \ll$ 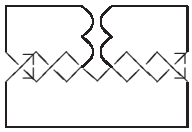 $\gg_{a^6+1}$

$+ yx \ll$ 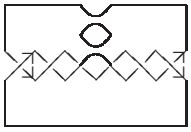 $\gg_{a^6+1} + y^2 \ll$ 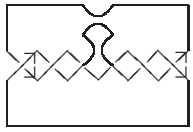 $\gg_{a^6+1}$

$= x^2 \ll O^2 \gg_{a^6+1} + xy \ll$ 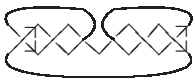 $\gg_{a^6+1}$

$+ yx \ll O^3 \gg_{a^6+1} + y^2 \ll O^2 \gg_{a^6+1}$

$= -x^2 + xy + yx - y^2 = -(x - y)^2.$

Theorem 6.3. Let D be an oriented marked graph diagram with h marked vertices, and let $L_+(D)$ be the positive resolution of D. Then

$$\ll D \gg_{a^6+1} = \epsilon(x - y)^h,$$

where $\epsilon = (-1)^{\#L_+(D)-1}$.

Proof. By (4.3),

$$\ll D \gg_{a^6+1} = \sum_{\sigma \in \mathcal{S}(D)} x^{\sigma(\infty)} y^{\sigma(0)} \ll D_\sigma \gg_{a^6+1} . \tag{6.11}$$

Let σ^* be the state assigning T_∞ to every marked vertex of D. Then $D_{\sigma^*} = L_+(D)$. By Lemma 6.1, $\ll D_{\sigma^*} \gg_{a^6+1} = (-1)^{\#L_+(D)-1} = \epsilon$. Since $\sigma^*(\infty) = h$ and $\sigma^*(0) = 0$, the state σ^* contributes ϵx^h in the right hand side of (6.11). Let σ be a state of D, which is obtained from σ^* by switching T_∞ and T_0 on k marked vertices. Then $\#D_\sigma - \#L_+(D) \equiv k \mod 2$, and by Lemma 6.1, $\ll D_\sigma \gg_{a^6+1} = (-1)^{\#D_\sigma - 1} = (-1)^{\#L_+(D)-1+k} = \epsilon(-1)^k$. Since $\sigma(\infty) = h - k$ and $\sigma(0) = k$, the contribution $x^{\sigma(\infty)} y^{\sigma(0)} \ll D_\sigma \gg_{a^6+1}$ of σ is $\epsilon(-1)^k x^{h-k} y^k$. Since every state σ is obtained from σ^* by choosing each subset of the marked vertices of D and switching T_∞ and T_0 there, we see that $\ll D \gg_{a^6+1} = \epsilon(x-y)^h$. □

Remark 6.4. From Theorem 6.3, we see that all information the invariant $\ll D \gg_{a^6+1}$ has is the number of marked vertices of D and the parity of $\#L_+(D)$. By this reason or by Propositions 5.4 and 5.5 with $\Delta(a) = 0$, we see that $\ll D \gg_{a^6+1}$ is invariant under Yoshikawa moves Γ_7 and Γ_8. In order to make it invariant under Yoshikawa move Γ_6, we may consider it up to multiplication by powers of $-x + y$ and $x - y$. However, this makes $\ll D \gg_{a^6+1}$ the same value for all D.

Suppose $m = 12$. Then for any positive integer μ,

$$\ll O^\mu \gg_{a^{12}+1} = 1 \tag{6.12}$$

and for any skein triple (D_+, D_-, D_0) of link diagrams,

$$-a^3 \ll D_+ \gg_{a^{12}+1} + a^{-3} \ll D_- \gg_{a^{12}+1} = (a^{-3} - a^3) \ll D_0 \gg_{a^{12}+1} . \tag{6.13}$$

Lemma 6.5. For any link diagram D, $\ll D \gg_{a^{12}+1} = 1$.

Proof. When we restrict $\ll \cdot \gg_{a^{12}+1}$ to the family of oriented link diagrams, it is an oriented link invariant satisfying (6.12) and (6.13). On the other hand, the constant function 1 is also such an invariant. Since the coefficients $-a^3$ and a^{-3} in the left hand side of (6.13) are units in $\mathbb{Z}[a^{-1}, a, x, y]/I(a^{12}+1)$, we have $\ll D \gg_{a^{12}+1} = 1$ for any link diagram D. □

Theorem 6.6. Let D be an oriented marked graph diagram with h marked vertices. Then

$$\ll D \gg_{a^{12}+1} = (x+y)^h.$$

Proof. By (4.3),

$$\ll D \gg_{a^{12}+1} = \sum_{\sigma \in \mathcal{S}(D)} x^{\sigma(\infty)} y^{\sigma(0)} \ll D_\sigma \gg_{a^{12}+1} .$$

By Lemma 6.5, for any σ, $\ll D_\sigma \gg_{a^{12}+1} = 1$. Since every state σ is obtained by choosing each subset of the marked vertices of D for assignment of T_∞, we see that $\ll D \gg_{a^{12}+1} = (x+y)^h$. □

Remark 6.7. By Theorem 6.6, the invariant $\ll D \gg_{a^{12}+1}$ is determined by the number of marked vertices. It is invariant under Yoshikawa moves Γ_7 and Γ_8. In order to make it invariant under Yoshikawa move Γ_6, we may consider it up to multiplication by powers of $x+y$. However, this makes $\ll D \gg_{a^{12}+1}$ the same value for all D.

Now we consider another case that $m = 9$.

Suppose $m = 9$. Then for any positive integer μ,

$$\ll O^\mu \gg_{a^9+1} = (a^{-6}+1+a^6)^{\mu-1} = \begin{cases} 1 & (\mu = 1) \\ 3^{\mu-2}(a^{-6}+1+a^6) & (\mu \geq 2) \end{cases}$$

and for any skein triple (D_+, D_-, D_0) of link diagrams,

$$\ll D_+ \gg_{a^9+1} - \ll D_- \gg_{a^9+1} = (a^3 - a^{-3}) \ll D_0 \gg_{a^9+1} .$$

Instead of studying $\ll D_+ \gg_{a^9+1}$, we here discuss a weaker version as follows.

Consider the ideal $I(a^9+1, a^{-6}+1+a^6)$ of $\mathbb{Z}[a^{-1}, a, x, y]$ generated by a^9+1 and $a^{-6}+1+a^6$. We denote by $\ll D_+ \gg^*_{a^9+1}$ the polynomial $\ll D \gg$ modulo the ideal $I(a^9+1, a^{-6}+1+a^6)$, i.e.,

$$\ll D \gg^*_{a^9+1} \;=\; \ll D \gg + I(a^9+1, a^{-6}+1+a^6) \;\in \mathbb{Z}[a^{-1}, a, x, y]/I(a^9+1, a^{-6}+1+a^6).$$

Note that the ideal $I(a^9+1, a^{-6}+1+a^6)$ is equal to the ideal $I(a^6 - a^3 + 1)$.

Then $\ll \cdot \gg^*_{a^9+1}$ is an invariant of oriented marked graphs satisfying that for any positive integer μ,

$$\ll O^\mu \gg^*_{a^9+1} = \begin{cases} 1 & (\mu = 1) \\ 0 & (\mu \geq 2) \end{cases} \tag{6.14}$$

and for any skein triple (D_+, D_-, D_0) of link diagrams,

$$\ll D_+ \gg^*_{a^9+1} - \ll D_- \gg^*_{a^9+1} = (a^3 - a^{-3}) \ll D_0 \gg^*_{a^9+1} . \tag{6.15}$$

Lemma 6.8. Let D be an oriented link diagram and let $\nabla[D](z)$ be the Conway polynomial. Then $\ll D \gg^*_{a^9+1} = \nabla[D](a^3 - a^{-3})$.

Proof. When we restrict $\ll \cdot \gg^*_{a^9+1}$ to the family of oriented link diagrams, it is an oriented link invariant satisfying (6.14) and (6.15). On the other hand, $\nabla[\cdot](a^3 - a^{-3})$ is also such an invariant. Thus we have $\ll D \gg^*_{a^9+1} = \nabla[D](a^3 - a^{-3})$. □

Theorem 6.9. Let D be an oriented marked graph diagram. Then

$$\ll D \gg^*_{a^9+1} = \sum_{\sigma \in \mathcal{S}(D)} x^{\sigma(\infty)} y^{\sigma(0)} \nabla[D_\sigma](a^3 - a^{-3}).$$

Proof. By (4.3),

$$\ll D \gg^*_{a^9+1} = \sum_{\sigma \in \mathcal{S}(D)} x^{\sigma(\infty)} y^{\sigma(0)} \ll D_\sigma \gg^*_{a^9+1} .$$

By Lemma 6.8, we have the result. □

Example 6.10. Consider the diagram 8_1 of a spun trefoil in Yoshikawa's table [21].

8_1

$\ll$ 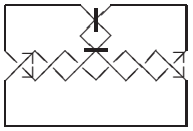 $\gg^*_{a^9+1}$

$= x^2 \ll$ 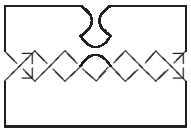 $\gg^*_{a^9+1} + xy \ll$ 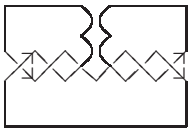 $\gg^*_{a^9+1}$

$+ yx \ll$ 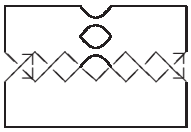 $\gg^*_{a^9+1} + y^2 \ll$ 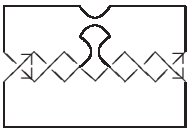 $\gg^*_{a^9+1}$

$= x^2 \ll O^2 \gg^*_{a^9+1} + xy \ll$ 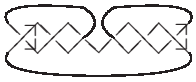 $\gg^*_{a^9+1}$

$+ yx \ll O^3 \gg^*_{a^9+1} + y^2 \ll O^2 \gg^*_{a^9+1}$

$= xy\nabla[$ 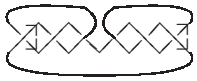 $](a^3 - a^{-3})$

$= 9xy.$

Remark 6.11. The polynomial $\ll D \gg^*_{a^9+1}$ $(\in \mathbb{Z}[a^{-1}, a, x, y]/I(a^9+1, a^{-6}+1+a^6))$ is not invariant under Yoshikawa moves $\Gamma_6, \Gamma'_6, \Gamma_7$ and Γ_8. When we evaluate it with $x = 1$ and $y = 1$, it becomes invariant under Γ_6 and Γ'_6. In Section 7 we will observe that $\ll D \gg^*_{a^9+1}$ $(\in \mathbb{Z}[a^{-1}, a, x, y]/I(a^9 + 1, a^{-6} + 1 + a^6))$ is an invariant when we restrict to "ribbon marked graphs".

7 Ribbon marked graphs

Let D be a marked graph diagram. We call a pair of marked vertices of D a *ribbon pair* if they are the vertices of a bigon in D and the markers are not parallel.

Definition 7.1. A marked graph diagram is called *ribbon* if the marked vertices are divided into ribbon pairs. A marked graph is called *ribbon* if there is a ribbon marked graph diagram presenting the marked graph.

For example, the marked graph diagrams 8_1 and 9_1 in Examples 4.5 and 4.6 are ribbon.

A surface-link is called *ribbon* if it is obtained from a trivial 2-link by surgery along some 1-handles attaching it. It is known that for any admissible ribbon marked graph diagram D, the surface-link $\mathcal{L}(D)$ presented by D is a ribbon surface-link, and conversely that for any ribbon surface-link $\mathcal{L}$ there is an admissible ribbon marked graph diagram D such that $\mathcal{L}(D)$ is equivalent to $\mathcal{L}$.

When D is ribbon, the positive resolution $L_+(D)$ and the negative resolution $L_-(D)$ are isotopic diagrams.

Let D be an oriented ribbon marked graph diagram presenting a ribbon 2-knot. Let n be the number of ribbon pairs of marked vertices. The number of marked vertices is $2n$, and $L_+(D)$ and $L_-(D)$ are diagrams of a trivial link with $n + 1$ components.

Theorem 7.2. Let D be an admissible oriented ribbon marked graph diagram with $2n$ marked vertices. If $\mathcal{L}(D)$ is a 2-knot, then $\ll D \gg^*_{a^9+1}$ is a multiple of $(xy)^n$, and $(xy)^{-n} \ll D \gg^*_{a^9+1}$ is determined from the equivalence class of the ribbon 2-knot.

Thus, the restriction of the invariant $\ll \cdot \gg^*_{a^9+1}$ of marked graphs to ribbon marked graphs presenting 2-knots is an invariant of ribbon 2-knots, up to multiplication by powers of xy.

Proof. (1) Assume that $n \geq 1$. Let σ_* (or σ_{**}, resp.) be the state of D assigning $T(\infty)$ (or $T(0)$, resp.) to every marked vertex. There is a unique state, say σ_0, in $\mathcal{S}(D) - \{\sigma_*, \sigma_{**}\}$ such that D_{σ_0} is a diagram of a knot. For any state σ in $\mathcal{S}(D) - \{\sigma_*, \sigma_{**}, \sigma_0\}$, D_σ is a disjoint union $D_{\sigma_0} \sqcup O^\mu$ for some $\mu = \mu(\sigma) \geq 1$. By Proposition 6.9,

$$\ll D \gg^*_{a^9+1} = \sum_{\sigma \in \mathcal{S}(D)} x^{\sigma(\infty)} y^{\sigma(0)} \nabla[D_\sigma](a^3 - a^{-3}) = x^{\sigma_0(\infty)} y^{\sigma_0(0)} \nabla[D_{\sigma_0}](a^3 - a^{-3}).$$

Since σ_0 assigns $T(\infty)$ to one marked vertex and $T(0)$ to another marked vertex for each ribbon pair of marked vertices, we have $\sigma_0(\infty) = \sigma_0(0) = n$. Thus

$$\ll D \gg^*_{a^9+1} = (xy)^n \nabla[D_{\sigma_0}](a^3 - a^{-3}).$$

Let K be the knot presented by the knot diagram D_{σ_0}. Then

$$(xy)^{-n} \ll D \gg^*_{a^9+1} = \nabla[K](a^3 - a^{-3}). \tag{7.16}$$

(2) When $n = 0$, D is a diagram of a trivial knot and $\ll D \gg^*_{a^9+1} = 1$. The 2-knot $\mathcal{L}(D)$ is a trivial 2-knot. Let K be the trivial knot. Then the same equality with (7.16) holds.

In either case (1) or (2), the ribbon 2-knot $\mathcal{L}(D)$ is equivalent to a 2-knot in a normal form in the sense of [8] such that it is symmetric with respect to $\mathbb{R}^3_0$ and the cross-sectional knot appearing at $\mathbb{R}^3_0$ is K. For such a knot K it is known that the Conway polynomial $\nabla[K](z)$ is determined from the equivalence class of the ribbon 2-knot. In particular, when the 2-knot is trivial, $\nabla[K](z) = 1$. Thus we see that $(xy)^{-n} \ll D \gg^*_{a^9+1}$ is determined from the equivalence class of the ribbon 2-knot $\mathcal{L}(D)$. □

Let $\varpi = \exp(\frac{2\pi\sqrt{-1}}{18}) \in \mathbb{C}$, a primitive 18th root of unity. Since $\varpi^9 + 1 = \varpi^{-6} + 1 + \varpi^6 = 0$, evaluation of $\ll D \gg^*_{a^9+1}$ with $a = \varpi$ is well-defined. Define $P^*_9(D)$ by

$$P^*_9(D) = \ll D \gg^*_{a^9+1} |_{a=\varpi} \quad \in \mathbb{C}[x, y].$$

Since $\varpi^{-3} = \varpi^3 = \sqrt{-3}$, it follows from Theorem 6.9 that

$$P^*_9(D) = \sum_{\sigma \in \mathcal{S}(D)} x^{\sigma(\infty)} y^{\sigma(0)} \nabla[D_\sigma](\sqrt{-3}).$$

From Theorem 7.2 and its proof, we obtain the following.

Theorem 7.3. Let D be an admissible oriented ribbon marked graph diagram with $2n$ marked vertices. If $\mathcal{L}(D)$ is a 2-knot, then $P^*_9(D)$ is a monomial $c(xy)^n$ and the coefficient $c \in \mathbb{C}$ is determined from the equivalence class of the ribbon 2-knot. When the 2-knot is a trivial 2-knot, then $c = 1$.

For example, for the marked graph diagram 8_1 in Example 4.5, the complex number c is 9. Thus we see that the 2-knot is not equivalent to a trivial 2-knot.

8 Proof of Lemma 5.2

Let G be an oriented tangled trivalent graph diagram in a 2-disk D^2 with the end points $s_1, \dots, s_6$ as shown in Figure 13 such that there are no connected components as diagrams in $\mathrm{Int}D^2$. If G has no crossings, then G forms a tiling, say G^*, of D^2, where we regard $\{s_1, \dots, s_6\}$ and $\{s_i s_{i+1} | 1 \leq i \leq 6\}$ as trivalent vertices and edges of the tiling G^*. Here $s_i s_{i+1}$ means an edge on ∂D^2 whose end points are s_i and s_{i+1}, and we assume $s_7 = s_1$.

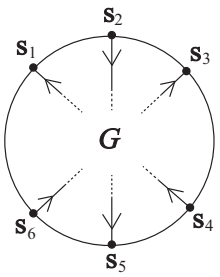

Figure 13: An oriented tangled trivalent graph diagram G in D^2

Let V, E and F be the numbers of the vertices, edges and faces of the tiling G^* of D^2, respectively, i.e., V and E are the number of vertices and edges of G^*, and F is the number of regions of $D^2 \backslash G^*$. For each integer $a \geq 1$, let F_a denote the number of faces of the tiling G^* that are a-gons. By the definition of oriented tangled trivalent graph diagram, there are only $2i$-gons ($i \geq 1$). Then

$$\begin{aligned}
F &= F_2 + F_4 + F_6 + F_8 + F_{10} + F_{12} + \cdots, \\
E &= \frac{1}{2}(6 + 2F_2 + 4F_4 + 6F_6 + 8F_8 + 10F_{10} + 12F_{12} + \cdots) = 3 + T, \\
V &= \frac{2}{3}E = \frac{2}{3}(3 + T) = 2 + \frac{2}{3}T, \text{ where } T := \sum_{i=1}^{\infty} iF_{2i}.
\end{aligned}$$

Considering the Euler characteristic of the tiling G^* of D^2, we have

$$\begin{aligned}
1 = V - E + F &= 2 + \frac{2}{3}T - (3 + T) + F = -1 - \frac{1}{3}T + F \\
&= -1 + \frac{1}{3}(2F_2 + F_4 - F_8 - 2F_{10} - 3F_{12} - \cdots).
\end{aligned}$$

This gives

$$2F_2 + F_4 - 6 = F_8 + 2F_{10} + 3F_{12} + \cdots. \tag{8.17}$$

For each i with $1 \leq i \leq 6$, we denote by $\overline{s_i s_{i+1}}$ a proper simple arc in D^2 whose end points are s_i and s_{i+1}. Note that when G has no 2-gons in $\mathrm{Int}D^2$, any 2-gon in G^*, if there exists, is $s_i s_{i+1} \cup \overline{s_i s_{i+1}}$ for some i.

Lemma 8.1. Let G be an oriented tangled trivalent graph diagram in D^2 with the end points $s_1, \dots, s_6$ as shown in Figure 13 such that there are no connected components as diagrams in $\mathrm{Int}D^2$. Suppose that G has no crossings, 2-gons and 4-gons in $\mathrm{Int}D^2$. Then the tiling G^* of D^2 is one of the tilings in Figure 14.

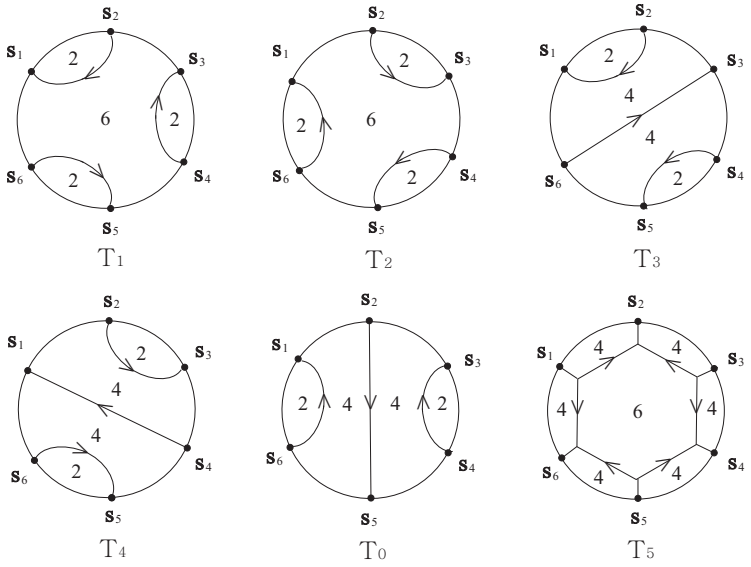

Figure 14: Tilings G^* of D^2 by G

Proof. It follows from (8.17) that

$$2F_2 + F_4 - 6 \geq 0. \tag{8.18}$$

Since there are no 2-gons in $\mathrm{Int}D^2$, we see that one of two edges of any 2-gon in G lies in the boundary ∂D^2. Since G has only trivalent vertices, any two distinct 2-gones cannot share a vertex $s_i (1 \leq i \leq 6)$ in common. This gives that $0 \leq F_2 \leq 3$.

Case I. Suppose $F_2 = 3$. The tiling G^* is T_1 or T_2 in Figure 14.

Case II. Suppose $F_2 = 2$. It follows from (8.18) that $F_4 \geq 2$.

(i) Suppose that the 2-gons are $\{s_1s_2 \cup \overline{s_1s_2}, s_3s_4 \cup \overline{s_3s_4}\}$ or they are in a position obtained by rotating $\{s_1s_2 \cup \overline{s_1s_2}, s_3s_4 \cup \overline{s_3s_4}\}$. Consider the case of $\{s_1s_2 \cup \overline{s_1s_2}, s_3s_4 \cup \overline{s_3s_4}\}$. Then edges $s_6s_1, \overline{s_1s_2}, s_2s_3, \overline{s_3s_4}, s_4s_5$ are edges of the same n-gon for some $n > 6$. Since any 4-gon of G^* must have s_5s_6 as an edge, we have $F_4 \leq 1$. This yields a contradiction. Similarly, when the 2-gons are in a position that is obtained by rotating $\{s_1s_2 \cup \overline{s_1s_2}, s_3s_4 \cup \overline{s_3s_4}\}$, we have a contradiction. Thus case (i) does not occur.

(ii) Suppose that the 2-gons are $\{s_1s_2 \cup \overline{s_1s_2}, s_4s_5 \cup \overline{s_4s_5}\}$ or they are in a position obtained by rotating $\{s_1s_2 \cup \overline{s_1s_2}, s_4s_5 \cup \overline{s_4s_5}\}$. Consider the case of $\{s_1s_2 \cup \overline{s_1s_2}, s_4s_5 \cup \overline{s_4s_5}\}$. Let A be a 4-gon in this tiling. Since there are no 4-gons in $\mathrm{Int}D^2$, one of the four edges of A have to be s_2s_3, s_3s_4, s_5s_6 or s_1s_6. If s_2s_3 or s_6s_1 is an edge of A, then $A = s_6s_1 \cup \overline{s_1s_2} \cup s_2s_3 \cup \overline{s_3s_6}$. Then the tiling is T_3 in Figure 14. If s_3s_4 or s_5s_6 is an edge of A, then by the same reason, the tiling is T_3. Thus we have T_3 in case this case. For the other cases, the tilings are obtained by rotating T_3, which are T_4 and T_0.

Case III. Suppose $F_2 = 1$. It follows from (8.18) that $F_4 \geq 4$.

Consider a case where the 2-gon is $s_1s_2 \cup \overline{s_1s_2}$.

(i) If s_2s_3 or s_6s_1 is an edge of a 4-gon A in G^*, then $A = s_6s_1 \cup \overline{s_1s_2} \cup s_2s_3 \cup \overline{s_3s_6}$. Since $F_4 \geq 4$, there are three 4-gons besides A. Each of them has edge

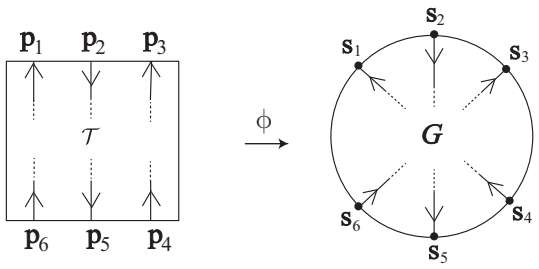

Figure 15: A homeomorphism $\phi : I^2 \to D^2$

s_3, s_4, s_4s_5, s_5s_6. However, a 4-gon having s_3s_4 or s_5s_6 is a 4-gon $s_5s_6 \cup \overline{s_6s_3} \cup s_3s_4 \cup \overline{s_4s_5}$. Then the tiling is T_3, and this contradicts to the assumption $F_2 = 1$. Thus this is not the case.

(ii) If neither s_2s_3 nor s_6s_1 is an edge of a 4-gon in G^*, then $F_4 \leq 3$. This contradicts to $F_4 \geq 4$. Thus this is not the case.

Case IV. Suppose $F_2 = 0$. It follows from (8.18) that $F_4 \geq 6$. Since each 4-gon has an edge in ∂D^2, we have T_5. □

Proof of Lemma 5.2. Let $\mathcal{T}$ be a 3-tangle diagram with the boundary (a) in Figure 7 such that there are no crossings, 2-gons and 4-gons and there are no connected components as diagrams in IntD^2. Let $p_1, \ldots, p_6$ be the end points of $\mathcal{T}$ and let $\phi : I^2 \to D^2$ be a homeomorphism from I^2 onto a 2-disk D^2 with $\phi(p_i) = s_i$ $(1 \leq i \leq 6)$. See Figure 15. Putting $G = \phi(\mathcal{T})$, we obtain the result from Lemma 8.1. □

9 Proof of Lemma 5.3

Let G be an oriented tangled trivalent graph diagram in a 2-disk D^2 with the end points $t_1, \ldots, t_8$ as shown in Figure 16 such that there are no connected components as diagrams in IntD^2. If G has no crossings, then G forms a tiling, say G^*, of D^2, where we regard $\{t_1, \ldots, t_8\}$ and $\{t_it_{i+1} \mid 1 \leq i \leq 8\}$ as trivalent vertices and edges of the tiling G, respectively. Here t_it_{i+1} means an edge of ∂D^2 whose end points are t_i and t_{i+1}, and we assume $t_9 = t_1$.

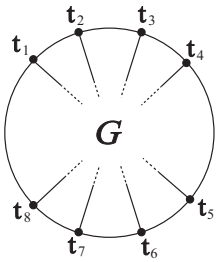

Figure 16: A 4-tangle of trivalent graph diagram

Let V, E and F be the numbers of the vertices, edges and faces of the tiling G^*, respectively. Then

$$F = F_2 + F_4 + F_6 + F_8 + F_{10} + F_{12} + F_{14} + \cdots,$$
$$E = \frac{1}{2}(8 + 2F_2 + 4F_4 + 6F_6 + 8F_8 + 10F_{10} + 12F_{12} + 14F_{14} + \cdots) = 4 + T,$$
$$V = \frac{2}{3}E = \frac{2}{3}(4 + T) = \frac{8}{3} + \frac{2}{3}T, \text{ where } T = \sum_{i=1}^{\infty} iF_{2i}.$$

Considering the Euler characteristic of the tiling G^* of D^2, we have

$$1 = V - E + F = \frac{8}{3} + \frac{2}{3}T - (4 + T) + F = -\frac{4}{3} - \frac{1}{3}T + F.$$

This gives

$$2F_2 + F_4 - 7 = F_8 + 2F_{10} + 3F_{12} + 4F_{14} + \cdots. \tag{9.19}$$

For each i with $1 \leq i \leq 8$, we denote by $\overline{t_i t_{i+1}}$ a proper simple arc in D^2 whose end points are t_i and t_{i+1}. Note that when G has no 2-gons in $\mathrm{Int}D^2$, any 2-gon in G^*, if there exists, is $t_i t_{i+1} \cup \overline{t_i t_{i+1}}$ for some i.

Lemma 9.1. Let G be an oriented tangled trivalent graph diagram in D^2 with the end points $t_1, \ldots, t_8$ as shown in Figure 16 such that there are no connected components as diagrams in $\mathrm{Int}D^2$. Suppose that G has no crossings, 2-gons and 4-gons in $\mathrm{Int}D^2$. Then the tiling G^* is one of the tilings in Figures 17, 18, 19, 20 and 21.

Proof. Since there are no 2-gons in $\mathrm{Int}D^2$, one of two edges of any 2-gon in G lies in ∂D^2. Since G^* has only trivalent vertices, any two distinct 2-gons cannot share a vertex t_i $(1 \leq i \leq 8)$ in common. This gives that $0 \leq F_2 \leq 4$.

Case I. Suppose $F_2 = 4$. Then G^* is one of the tilings shown in Figure 17.

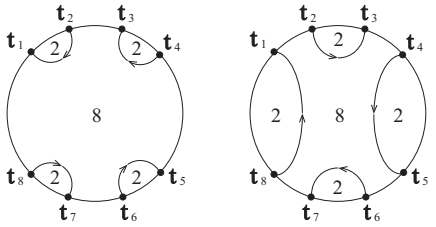

Figure 17: $F_2 = 4$

Case II. Suppose $F_2 = 3$. It follows from (9.19) that $0 \leq F_8 \leq F_4 - 1$. So $F_4 \geq 1$.

(i) Suppose that the three 2-gons are $\{t_1t_2 \cup \overline{t_1t_2}, t_3t_4 \cup \overline{t_3t_4}, t_5t_6 \cup \overline{t_5t_6}\}$ or they are in a position obtained by rotating $\{t_1t_2 \cup \overline{t_1t_2}, t_3t_4 \cup \overline{t_3t_4}, t_5t_6 \cup \overline{t_5t_6}\}$.

Consider the case of $\{t_1t_2 \cup \overline{t_1t_2}, t_3t_4 \cup \overline{t_3t_4}, t_5t_6 \cup \overline{t_5t_6}\}$. Edges $t_8t_1, \overline{t_1t_2}, t_2t_3, \overline{t_3t_4}$, $t_4t_5, \overline{t_5t_6}, t_6t_7$ are edges of the same n-gon for some $n \geq 8$. Thus by (9.19), we have $F_4 \geq 2$. On the other hand, any 4-gon of G^* has t_7t_8 as an edge. Thus $F_4 \leq 1$. This is a contradiction. In the other cases of (i), we have a contradiction. Thus the case (i) does not occur.

(ii) Suppose that the three 2-gons are $\{t_1t_2 \cup \overline{t_1t_2}, t_3t_4 \cup \overline{t_3t_4}, t_6t_7 \cup \overline{t_6t_7}\}$ or they are in a position obtained by rotating $\{t_1t_2 \cup \overline{t_1t_2}, t_3t_4 \cup \overline{t_3t_4}, t_6t_7 \cup \overline{t_6t_7}\}$.

Consider the case of $\{t_1t_2 \cup \overline{t_1t_2}, t_3t_4 \cup \overline{t_3t_4}, t_6t_7 \cup \overline{t_6t_7}\}$. Edges $t_8t_1, \overline{t_1t_2}, t_2t_3, \overline{t_3t_4}$, t_4t_5 are edges of the same n-gon for some $n \geq 6$. Since $F_4 \geq 1$, there is a 4-gon A in G^*. Since A has t_5t_6 or t_7t_8 as an edge, we have $A = t_5t_6 \cup \overline{t_6t_7} \cup t_7t_8 \cup \overline{t_8t_5}$. Then G^* is one of the tilings in Figure 18. In the other cases of (ii), we have the other tilings in Figure 18.

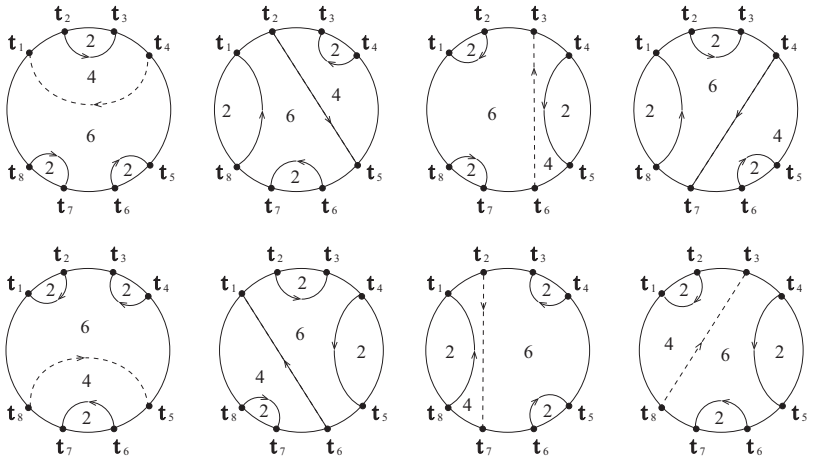

Figure 18: $F_2 = 3$

Case III. $F_2 = 2$. It follows from (9.19) that $0 \leq F_8 \leq F_4 - 3$ and so $F_4 \geq 3$.

(i) Suppose that the 2-gons are $\{t_1t_2 \cup \overline{t_1t_2}, t_3t_4 \cup \overline{t_3t_4}\}$ or in a position obtained by rotating them. Consider the case of $\{t_1t_2 \cup \overline{t_1t_2}, t_3t_4 \cup \overline{t_3t_4}\}$. Edges $t_8t_1, \overline{t_1t_2}, t_2t_3, \overline{t_3t_4}, t_4t_5$ are edges of the same n-gon for some $n \geq 6$. It implies $F_4 \leq 1$ as before. This contradicts to $F_4 \geq 3$. We have a contradiction in other cases of (i). Thus the case (i) does not occur.

(ii) Suppose that the 2-gons are $\{t_1t_2 \cup \overline{t_1t_2}, t_4t_5 \cup \overline{t_4t_5}\}$ or in a position obtained by rotating them. Consider the case of $\{t_1t_2 \cup \overline{t_1t_2}, t_4t_5 \cup \overline{t_4t_5}\}$.

(a) If t_2t_3 or t_8t_1 is an edge of a 4-gon, then the 4-gon is $t_8t_1 \cup \overline{t_1t_2} \cup t_2t_3 \cup \overline{t_3t_8}$. Edges $t_7t_8, \overline{t_8t_3}, t_3t_4, \overline{t_4t_5}, t_5t_6$ are edges of the same n-gon for some $n \geq 6$. Then another 4-gon, if there exists, must have t_6t_7 as an edge. Thus $F_4 \leq 2$, which contradicts to $F_4 \geq 3$.

(b) If t_3t_4 or t_5t_6 is an edge of a 4-gon, then by the same argument with (a), we have a contradiction.

By (a) and (b), if there is a 4-gon then it has t_6t_7 or t_7t_8. Thus $F_4 \leq 2$, which contradicts to $F_4 \geq 3$. Therefore we see that (ii) does not occur.

(iii) Suppose that the 2-gons are $\{t_1t_2 \cup \overline{t_1t_2}, t_5t_6 \cup \overline{t_5t_6}\}$ or in a position obtained by rotating them. Consider the case of $\{t_1t_2 \cup \overline{t_1t_2}, t_5t_6 \cup \overline{t_5t_6}\}$.

If none of $t_2t_3, t_4t_5, t_6t_7, t_8t_1$ is an edge of a 4-gon, then $F_4 \leq 2$, which contradicts to $F_4 \geq 3$. Thus, at least one of them is an edge of a 4-gon. Assume that t_2t_3 is so. Then $t_8t_1 \cup \overline{t_1t_2} \cup t_2t_3 \cup \overline{t_3t_8}$ is a 4-gon. Beside of this 4-gon, there are at least two 4-gons. Since one of them has t_4t_5 or t_6t_7 as an edge, it is the 4-gon $t_4t_5 \cup \overline{t_5t_6} \cup t_6t_7 \cup \overline{t_7t_4}$. Then we have a tiling in Figure 19. When one of t_4t_5, t_6t_7, t_8t_1 is an edge of a 4-gon,

we have the same tiling. For the other cases of (iii), we have a tiling by rotation. Thus the possible tilings are shown in the figure.

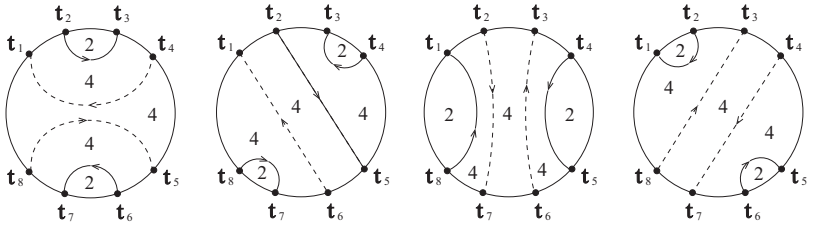

Figure 19: $F_2 = 2$

Case IV. Suppose $F_2 = 1$. It follows from (9.19) that $F_4 \geq 5$. Consider the case that the 2-gon is $t_1t_2 \cup \overline{t_1t_2}$. Edges $t_8t_1, \overline{t_1t_2}, t_2t_3$ are edges of the same n-gon, say A, for some $n \geq 4$.

(i) Suppose that A is a 4-gon. Namely, $A = t_8t_1 \cup \overline{t_1t_2} \cup t_2t_3 \cup \overline{t_3t_8}$ is a 4-gon in G^*. Besides A, there must be at least four 4-gons in G^*. Since each of which has one of $t_3t_4, t_4t_5, t_5t_6, t_6t_7, t_7t_8$ as an edge. Thus at least one of t_3t_4, t_7t_8 is an edge of a 4-gon. Then $A' := t_3t_4 \cup \overline{t_4t_7} \cup t_7t_8 \cup \overline{t_8t_3}$ is a 4-gon in G^*. Besides A, A', there must be at least four 3-gons in G^*. Since each of which has one of t_4t_5, t_5t_6, t_6t_7 as an edge. Then $A'' := t_4t_5 \cup \overline{t_5t_6} \cup t_6t_7 \cup \overline{t_7t_4}$ is a 4-gon in G^*. Then t_5t_6 is an edge of a 2-gon and we have $F_4 = 3$. This contradicts to $F_4 \geq 5$.

(ii) Suppose that A is a 6-gon. Since $F_4 \geq 5$ and since each 4-gon has one of $t_3t_4, t_4t_5, t_5t_6, t_6t_7, t_7t_8$ as an edge, the tiling G^* must be one of the tilings in Figure 20.

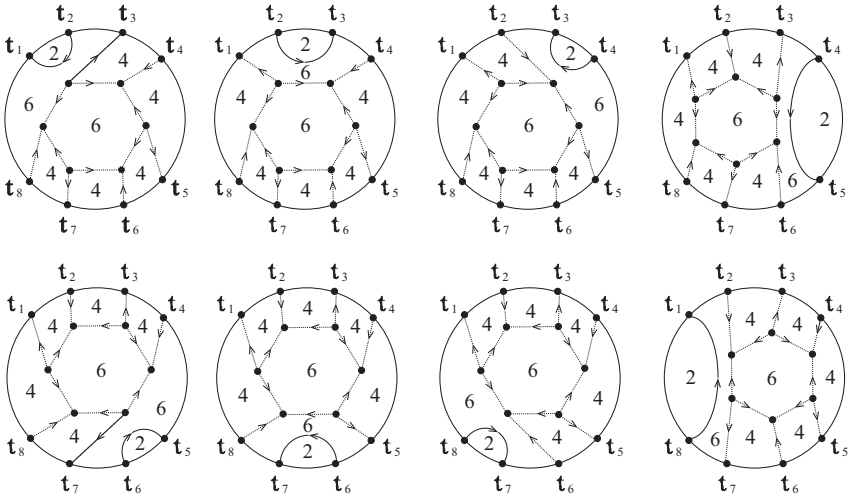

Figure 20: $F_2 = 1$

(iii) Suppose that A is an n-gon with $n \geq 8$. Then by (9.19) we have $F_4 \geq 6$. On the other hand, since each 4-gon has one of $t_3t_4, t_4t_5, t_5t_6, t_6t_7, t_7t_8$ as an edge, $F_4 \leq 5$. This is a contradiction. Thus (iii) does not occur.

Case V. Suppose $F_2 = 0$.

(i) Suppose $F_k = 0$ for all $k \geq 8$. It follows from (9.19) that $F_4 = 7$. The seven 4-gons consecutively appear along ∂D^2. There are seven edges that are edges of the seven 4-gons and they are disjoint from ∂D^2. The seven edges are edges of the same n-gon for some $n \geq 8$. This contradicts the hypothesis.

(ii) Suppose $F_k \neq 0$ for some $k \geq 8$. It follows from (9.19) that $F_4 \geq 8$. Since each 4-gon has an edge in ∂D^2, the tiling G is as in Figure 21. □

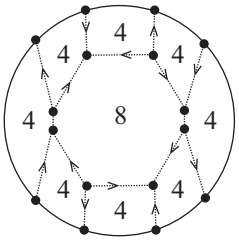

Figure 21: $F_2 = 0$

Now we are in a position to complete the proof of Lemma 5.3.

Proof of Lemma 5.3. Let $\mathcal{T}$ be a 4-tangle diagram with the boundary (a) in Figure 7 such that there are no crossings, 2-gons and 4-gons cut that there are no connected components as diagrams in IntD^2. Let $q_1, \ldots, q_8$ be the end points of $\mathcal{T}$ and let $\phi : I^2 \to D^2$ be a homeomorphism from I^2 onto a 2-disk D^2 with $\phi(q_i) = t_i (1 \leq i \leq 8)$. See Figure 22. Putting $G = \phi(\mathcal{T})$, we obtain the result from Lemma 9.1. □

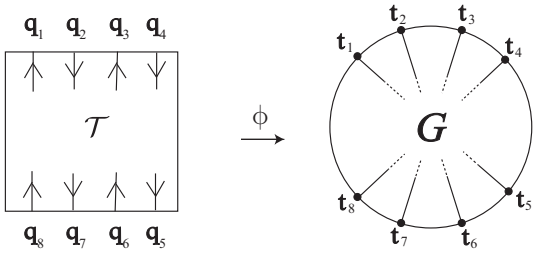

Figure 22: A homeomorphism $\phi : I^2 \to D^2$

Acknowlegements

The second and the third authors were supported by JSPS KAKENHI Grant Numbers 24244005 and 26287013. The fourth author was supported by Basic Science Research Program through the National Research Foundation of Korea (NRF) funded by the Ministry of Education, Science and Technology (2013R1A1A2012446).

References

[1] M. Asada, An unknotting sequence for surface-knots represented by ch-diagrams and their genera, *Kobe J. Math.* **18** (2001), 163–180.

[2] P. Freyd, D. Yetter, J. Hoste, W. B. R. Lickorish, K. Millett and A. Ocneanu, A new polynomial invariant of knots and links, Bull. Amer. Math. Soc. (N.S.) **12** (1985), no. 2, 239–246.

[3] Y. Joung, S. Kamada and S. Y. Lee, Applying Lipson's state models to marked graph diagrams of surface-links, *J. Knot Theory Ramifications* **24** (2015), no. 10, 1540003 (18 pages).

[4] Y. Joung, J. Kim and S. Y. Lee, Ideal coset invariants for surface-links in $\mathbb{R}^4$, *J. Knot Theory Ramifications* **22** (2013), no. 9, 1350052 (25 pages).

[5] S. Kamada, Braid and Knot Theory in dimension Four, Mathematical Surveys and Monographs **95**, American Mathematical Society, Providence, RI, 2002.

[6] S. Kamada, J. Kim and S. Y. Lee, Computations of quandle cocycle invariants of surface-links using marked graph diagrams, *J. Knot Theory Ramifications* **24** (2015), no. 10, 1540010 (35 pages).

[7] A. Kawauchi, A survey of knot theory, Birkhäuser Verlag, Basel, 1996.

[8] A. Kawauchi, T. Shibuya and S. Suzuki, Descriptions on surfaces in four-space, I; Normal forms, *Math. Sem. Notes Kobe Univ.* **10** (1982), 75–125.

[9] J. Kim, Y. Joung and S. Y. Lee, On the Alexander biquandles of oriented surface-links via marked graph diagrams, *J. Knot Theory Ramifications* **23** (2014), no. 7, 1460007 (26 pages).

[10] J. Kim, Y. Joung and S. Y. Lee, On generating sets of Yoshikawa moves for marked graph diagrams of surface-links, *J. Knot Theory Ramifications* **24** (2015), no. 4, 1550018 (21 pages).

[11] C. Kearton and V. Kurlin, All 2-dimensional links in 4-space live inside a universal 3-dimensional polyhedron, *Algebraic & Geometric Topology* **8** (2008), 1223–1247.

[12] G. Kuperberg, The Quantum G_2 link invariant, *International Jounal of Mathematics* **5** (1994), no. 1, 61–85.

[13] S. Y. Lee, Invariants of surface-links in $\mathbb{R}^4$ via classical link invariants. Intelligence of low dimensional topology 2006, pp. 189–196, Ser. Knots Everything, **40**, World Sci. Publ., Hackensack, NJ, 2007.

[14] S. Y. Lee, Invariants of surface-links in $\mathbb{R}^4$ via skein relation, *J. Knot Theory Ramifications* **17** (2008), no.4, 439–469.

[15] S. Y. Lee, Towards invariants of surfaces in 4-space via classical link invariants, *Trans. Amer. Math. Soc.* **361** (2009), no. 1, 237–265.

[16] S. Y. Lee, Polynomial invariants for surface-links from the Jones-Kauffman polynomial, Preprint.

[17] S. J. Lomonaco, Jr., The homotopy groups of knots I. How to compute the algebraic 2-type, *Pacific J. Math.* **95** (1981), no. 2, 349–390.

[18] N. Yu. Reshetikhin and V. G. Turaev, Ribbon graphs and their invariants derived from quantum groups. *Comm. Math. Phys.* **127** (1990), no. 1, 1–26.

[19] M. Soma, Surface-links with square-type ch-graphs, Proceedings of the First Joint Japan-Mexico Meeting in Topology (Morelia, 1999), *Topology Appl.* **121** (2002), 231–246.

[20] F. J. Swenton, On a calculus for 2-knots and surfaces in 4-space, *J. Knot Theory Ramifications* **10** (2001), no. 8, 1133–1141.

[21] K. Yoshikawa, An enumeration of surfaces in four-space, *Osaka J. Math.* **31** (1994), no. 3, 497–522.